Journal of the Meteorological Society of Japan

EARLY ONLINE RELEASE

The DOI for this manuscript is

DOI:10.2151/jmsj.2025-027

J-STAGE Advance published date: May 21, 2025

Arctic amplification in the past, present, and future: A review for the challenge to the integrative understanding of its mechanism

Masakazu YOSHIMORI[1], **Takao KAWASAKI, Ayako ABE-OUCHI, and Hiroyasu HASUMI**

Atmosphere and Ocean Research Institute
The University of Tokyo, Kashiwa, Japan

May 7, 2025 (accepted by *Journal of the Meteorological Society of Japan*)

----

1) Corresponding author: Masakazu Yoshimori, Atmosphere and Ocean Research Institute
The University of Tokyo, 5-1-5, Kashiwanoha, Kashiwa, Chiba 277-8568 JAPAN
Email: masakazu@aori.u-tokyo.ac.jp
Tel: +81-4-7136-4380

Abstract

It is well known that the Arctic is warming at a much faster rate than other regions of the world. Within the context of the state of modern climate conditions, enhanced Arctic warming has also been investigated in paleoclimate reconstructions and simulations during relatively warm periods. Since sea ice plays a central role in generating these geographical patterns of warming amplification, a thorough understanding of both atmospheric and oceanic dynamics is important. Studies have suggested that several commonalities may exist in the mechanisms underlying the amplification of Arctic warming across different historical periods, despite the diverse nature of external forcings. In this review, we consolidate modern and paleoclimatic perspectives to reveal challenges posed to an integrated understanding of the mechanisms driving the amplification of Arctic warming in the past, present, and future. An emphasis is placed on large-scale atmospheric and oceanic processes. Important unresolved issues and avenues for further investigation are also discussed from the climate system point of view.

Keywords Arctic amplification; polar amplification; climate change; paleoclimate

1. Introduction

The Arctic region is warming at a much faster rate than other regions of the world (Fig.1). The rate of increase in surface air temperature (SAT) in the Arctic is several times as large as the global mean over recent decades, although the exact rate depends on the period, the definition of the Arctic, and the datasets used (Rantanen et al. 2022). This geographic signature of warming is referred to as Arctic amplification (AA), and is characterized by other striking features, such as strong warming in the relatively cold season and near the surface. Prior to empirical confirmation of the emergence of AA in the real world (Serreze and Francis 2006), early studies on global climate modeling forecasted the phenomenon of polar amplification in warming patterns (Manabe and Wetherald 1975; Manabe and Stouffer 1979). The mechanism of AA is scientifically intriguing but challenging because it involves interactions of the climate system components, such as the atmosphere, ocean, and sea ice. The AA is also societally relevant because it may impact other parts of the world, including the climate, weather, and extreme events at mid-latitudes.

In the previous decade or so, several review articles on Arctic warming and AA have been published (Goosse et al. 2018; Previdi et al. 2021; Semenov 2021; Serreze and Barry 2011; Taylor et al. 2022). These investigations have primarily focused on extant changes in the Arctic environment with some insights derived through numerical experiments. However, since the polar amplification of climate change is known to have occurred frequently throughout the Earth's history, a concerted effort to synthesize the characteristics of these events over time may increase the confidence with which we can predict changes in the future. Consequently, we also review studies on climate change at different times to clarify the large-scale processes associated with AA and to frame the topic using a much broader perspective than is typically employed. Therefore, the methodological approach employed in this review is distinct from existing review articles, while offering insights that are both novel and complementary.

This review aims to present the current state of our understanding of mechanisms for Arctic warming amplification in response to external forcings in the past, present, and future. On the other hand, it would reveal that their integrative understanding is not mature, posing challenges. In section 2, the observed Arctic change is briefly summarized, followed by studies distinguishing externally forced change (EX) and internal variability (IV). The review then covers the local feedback processes amplifying the Arctic response and the remote influence from lower latitudes on the Arctic changes. Studies on paleoclimate focusing on three different periods are reviewed in section 3. The final goal of this review is to discuss the focal points for formulating an integrated understanding of the mechanisms underlying AA that may be an inherent property of the response of climate systems to external forcing. Relevant discussions are made in Section 4, followed by the summary in Section 5.

2. Modern-climate perspectives

2.1 Observed changes in the Arctic surface climate

The current 'thermal' state of the Arctic, including air temperature, permafrost temperature, terrestrial snow cover, river ice, sea ice, and land ice, is concisely summarized by the Arctic Monitoring and Assessment Program (AMAP) reports (e.g., AMAP 2021). Fig. 2 shows the time series of three thermally sensitive indices. Independently compiled, multiple gridded surface temperature data and global atmospheric reanalysis datasets provide convincing evidence of AA (Figs. 1 and 2). These datasets incorporate numerous observational records in their construction, including those from land stations, ships, and satellites. Rantanen et al. (2022) reported that the speed of the Arctic average warming from 1979 to 2021 was about four times faster than the global average warming.

The reduction in sea ice cover is the most striking feature of Arctic warming. Continuous satellite microwave monitoring[1] from 1978 provides high confidence in this recognition (e.g., Comiso and Nishio 2008, Kern et al. 2020, Kern et al. 2019). Box et al. (2021) reported that the Arctic sea-ice extent diminished by 43% from 1979 to 2019. Estimating sea ice thickness (and snow depth on top of it) using satellite altimeters has proven challenging (e.g., Kacimi and Kwok 2022, Kwok et al. 2020). Nevertheless, compared with submarine sonar records, Kwok (2018) estimated that the sea ice thickness decreased by about 2 m from 1958–1976 to 2011–2018 in six Arctic regions (Chukchi Cap, Beaufort Sea, Canada Basin, North Pole, Nansen Basin, and Eastern Arctic). Decreases in multiyear ice cover as well as increases in

[1] These instruments include the Scanning Multichannel Microwave Radiometer (SMMR), the Special Sensor Microwave/Imager (SSM/I), and the Advanced Scanning Microwave Radiometer (AMSR-E and AMSR2).

ice velocity and the length of the ice melt season were also reported (Carmack et al. 2015).

Arctic Ocean changes are not limited to sea ice; they have also been observed in subsurface ocean temperatures and salinity. The terms “Atlantification”, “Pacification”, and “borealization” have been introduced to describe the rapid changes in parts of the Arctic Ocean that have become similar to parts of the mid-latitude oceans (Polyakov et al. 2020b). The term “Arctic Ocean amplification” was coined by Shu et al. (2022) to describe an increase in the Arctic Ocean temperature that is more pronounced than the global average. We elaborate on these observed changes in Section 2.4.2.

Optical images from satellites directly capture the land-snow cover change, whereas there are complicated steps to estimate the land-snow mass change (Box et al., 2021; Estilow et al. 2015). Box et al. (2021) reported that the extent of the Arctic's May-to-June land snow cover diminished by 21% from 1971 to 2019. They also reported that river discharge to the Arctic Ocean increased by 8% from 1971 to 2019. Using a land surface model that simulates surface and subsurface runoffs and a river routing model, Park et al. (2024) attributed the increased and decreased discharge to the Arctic Ocean in May-June and July-August, respectively, to the earlier seasonal snow melting.

2.2 Role of internal variability

While the primary subject of this review is understanding how Arctic warming is amplified in response to external forcings, understanding the IV is highly relevant. Quantifying the IV component is essential to correctly interpret the observed changes and impose constraints isolating the EX component. Large ensemble simulations of more than a few dozen members became available about a decade ago, allowing us to separate IV and EX components. As the phase of the IV component is not fixed to a particular time, the ensemble mean and variance may be considered as the EX and IV components, respectively. It was estimated that the EX component of Arctic warming is about threefold in contrast to the observed fourfold speed of global warming over the past four decades (Sweeney et al. 2023, Zhou et al. 2024).

A similar exercise was made for the change in Arctic sea-ice extent over the past decades. Shen et al. (2024) evaluated the IV component as 17.8% (1979-2014) and 8% (1958-2017) in the total variances, much smaller than those estimated previously (Ding et al. 2018, England et al. 2019, Kay et al. 2011), after statistically correcting the underestimated forced response in models. Dörr et al. (2023) attributed approximately 90% of Arctic sea-ice loss in winter to external forcing. Focusing on the Barents-Kara Sea ice loss in winter, Siew et al. (2024) attributed about 70% of the average trends of 20-year running windows over the past four decades to anthropogenic forcing, pointing out the relevance to local dipole sea-level pressure patterns. On the other hand, Li et al. (2022) argue the significant IV contribution of up to 60% to the upper Arctic Ocean warming from 2000 to 2018.

Different studies suggest that a different mode of variability is responsible for the IV component of Arctic temperature changes: Atlantic multidecadal variability (AMV) (Chen and Dai 2024, Miles et al. 2014), a local Arctic mode of variability through atmosphere-sea ice interaction (Liu et al. 2022, Zhou et al. 2024), and interdecadal Pacific variability (IPV) (Screen and Francis 2016, Zhou et al. 2024). It is worth noting that both AMV and IPV as well as natural forcing are suggested to be responsible for the early 20th-century AA (Aizawa et al. 2021; Svendsen et al. 2018, Tokinaga et al. 2017; Yamanouchi 2011). While sea surface temperature (SST) in the Chukchi and Bering Seas is under the strong influence of Pacific decadal variability, it is interesting that the record-high autumn value was achieved by atmospheric blocking events, indicating the important role of short-term variabilities (Kodaira et al. 2020). The competing effect of atmospheric forcing and ocean advection on seasonal sea ice evolution in this region was also reported (Nakanowatari et al. 2022).

Other studies reported the tropical influence (Henderson et al. 2021). Zhang et al. (2023) showed the concentrated filamentary moisture flow, popularly known as atmospheric river (AR), is increasing in the Barents-Kara Sea, being forced partially by the IV at low latitudes, which in turn slows down the sea ice growth in winter. Ding et al. (2014) argue that the remote influence from lower latitudes through the planetary Rossby waves is responsible for the observed warming in northeastern Canada and Greenland, and Ding et al. (2018) stress the importance of low-latitude influence for the Arctic sea-ice loss. The elaboration on the link between the IV and regional inhomogeneity of Arctic warming is necessary.

The complication arises because the modes of variability are not purely internal but may also be modulated by external forcings. Nevertheless, the role of IV is expected to diminish in the quasi-equilibrium AA response, which is more relevant to paleoclimate and century-scale future changes.

2.3 Arctic feedback processes

2.3.1 Quantifying the relative contribution

Our understanding of the polar feedback processes that contribute to the enhancement of Arctic warming has progressed considerably over the last decade (Goosse et al. 2018; Previdi et al. 2021; Taylor et al. 2022). It is widely acknowledged that alterations in sea ice cover play a central role in driving AA (Dai et al. 2019; Screen and Simmonds 2010; Serreze et al. 2009). Early modeling studies have already proposed that a variety of processes, including changes in albedo due to ice/snow melting, seasonal atmosphere-ocean heat exchange, and weak vertical mixing due to well-developed stratification in the lower troposphere, play important roles in producing the features of AA described in the Introduction (Manabe and Wetherald 1975; Manabe and Stouffer 1979). Numerical simulations using methods that suppress specific feedback processes (“online suppression method” described by Bony et al. (2006)) have improved our understanding of the emergence of AA, by isolating the effect of surface albedo (Alexeev 2003; Alexeev et al. 2005; Graversen and Wang 2009; Hall 2004; Langen et al. 2012; Lu and Cai 2010), vertical mixing in the lower troposphere (Bintanja et al. 2011; Bintanja et al. 2012), clouds (Middlemas et al. 2020; Vavrus 2004), and water vapor (Hall and Manabe 1999; Schneider et al. 1999). It has also been demonstrated that weaker vertical mixing in the lower troposphere leads to an increase in AA, and that AA can occur even without changes in surface albedo. However, because of the non-additive nature of feedback processes through mutual interaction, these results have been difficult to verify empirically and to integrate within existing frameworks.

The quantification of the relative importance of polar feedback processes has conventionally been based primarily on an energy balance framework. The energy balance at the surface is linked to surface temperature changes more directly than at other levels through upwelling longwave radiation. However, quantifying the contribution of atmospheric heat transport (AHT) is not straightforward (Laîné et al. 2016; Lu and Cai 2009b; Pithan and Mauritsen 2014). On the other hand, while the energy balance at the top of the atmosphere (TOA) can be used to quantify the combined effect of AHT and ocean heat transport (OHT), conversion of the TOA energy flux to temperature change is indirect and assumes a vertically uniform (Planck) response (Crook et al. 2011; Hahn et al. 2021; Pithan and Mauritsen 2014). In principle, observations can provide the foundation for corroborating these estimates. While energy balance analyses at a single level can be used to quantify the effect of lapse-rate feedback (i.e., deviation from the vertically uniform temperature change), such analyses do not explain which processes contribute to the enhanced near-surface warming, which is an important feature of AA (Lu and Cai 2009a). However, solving the simultaneous equations for the energy balance at the surface and at every atmospheric level compensates for this deficit (Lu and Cai 2009a; Yoshimori et al. 2014a, 2014b).

While the exact decomposition of feedback to individual components and their relative roles in AA differ according to the analytical method used (Sejas et al. 2021; Feldl et al. 2020), the following general understanding has emerged. The reduction of sea ice cover increases the absorption of shortwave radiation in summer, causing a small rise in the temperature of the ocean mixed layer due to the relatively large heat capacity of seawater (Fig. 3, bottom). When the cold season arrives, excessive heat is released into the atmosphere through the expanded area of open water. The strong atmospheric near-surface stratification that occurs in the cold season confines the warming to within a relatively shallow atmospheric layer (Fig. 3, top). We note that the radiative effect of the bottom-heavy vertical profile in temperature change corresponds to the positive lapse-rate feedback. Recent studies have argued, however, that strong atmospheric stratification is not a necessary condition of strong positive lapse-rate feedback based on the analysis of spatial variations and numerical experiments (Boeke et al. 2021; Dai and Jenkins 2023; Jenkins and Dai 2021; Jenkins and Dai 2022). Additionally, the nonlinearity of the Stefan-Boltzmann law has the effect of raising the level of warming with a given energy imbalance at the cold climate state because less longwave radiation is emitted per unit degree of warming at lower temperatures (Ohmura 1984, 2012). In climate models, negative shortwave cloud feedback in summer and positive longwave cloud feedback in winter also appear to be important, but the contribution of the cloud response in the real world is uncertain. We elaborate this uncertainty in the next section. Other studies reported that the amplification effects from the nonlinearity of the radiation law or cloud radiative feedback might be diminished by other feedback mechanisms when the effect is identified using the online suppression method, which permits the “compensation” of feedback effects (Henry and Merlis 2019; Middlemas et al. 2020). Nevertheless, amplifying effects on Arctic warming through the annual cycle have also been verified using Coupled Model Intercomparison Project Phase 6 (CMIP6) models (Hu et al. 2022). Hereafter, we refer to this amplification mechanism, which operates through seasonal modulation of energy exchange at the sea surface[2] (Fig. 3), as the ‘seasonal modulation mechanism’.

2.3.2 Recent focus on uncertainties associated with clouds and aerosols

Clouds are essential ingredients affecting the Earth’s radiation budget. How they respond to climate forcing is one of the largest sources of uncertainty in the Arctic and other regions because microphysical and dynamical cloud processes are very complex (Curry et al. 1996). More specifically, our knowledge is limited on how cloud amount, altitude, and type change under the changing surface conditions of ice cover, marginal ice zone, and open water. In the Arctic, low-level clouds prevail throughout the year (e.g., Gierens et al. 2020, Griesche et al. 2024; Intrieri et al. 2002; Shupe et al. 2001), and recent satellite observations with active sensors distinguish the phase of cloud particles, revealing that mixed-phase clouds containing a significant amount of supercooled liquid water are common (Kay et al. 2016). Although this topic is important, comprehensive reviews or discussions on individual

[2] A closed energy budget analysis of the present-day, annual-cycle climatology for the Arctic atmosphere-ocean system was presented by Mayer et al. (2019). Their analysis showed that the ocean absorbs heat during the summer and releases it to the atmosphere during the winter.

elementary processes and their evaluations are beyond the scope of this review. Readers are referred to Devasthale et al. (2020) and Tan et al. (2023).

Kay et al. (2016) stressed the important role of mixed-phase clouds in the Arctic climate. Here, we highlight the cloud-phase feedback that has recently drawn significant attention (e.g., Sagoo et al. 2021; Sherriff-Tadano et al. 2023; Tan et al. 2016; Zelinka et al. 2020), and some of the uncertainties associated with aerosols. It has been known for some time that cloud phase change acts as negative feedback in climate changes where an increase in cloud droplets at the expense of ice crystals leads to an increase in both the reflectivity and lifetime of clouds, which in turn reduces the shortwave radiation absorbed by the Earth (Tsushima et al. 2006, Yoshimori et al. 2009). Tan and Storelvmo (2019) suggest that this mechanism may act as positive feedback in the Arctic because an increase in cloud lifetime leads to an increase in the downwelling longwave radiation reaching the Earth's surface, i.e., the greenhouse effect. Consequently, the cloud feedback associated with phase change may enhance Arctic warming in winter with little insolation, contributing to AA. These mechanisms remain to be verified more rigorously by empirical observations, however (Morrison et al. 2011a).

Given the rapid and great loss of sea ice in the Arctic, the ice cover and cloud interaction is another important topic. Kay et al. (2016) concluded that there is little response of clouds to the change from an ice-covered ocean to an ice-free ocean during summer. On the other hand, they also concluded that the sea ice loss leads to an increase in turbulent moisture fluxes, a deepening of the boundary layer, and an increase in cloud cover during fall. Their conclusions were supported by a recent study based on satellite observations, concluding that the cloud feedback to sea ice loss is negative in spring and positive in fall and winter (Taylor and Monroe, 2023). Again, the mechanisms remain to be elaborated further by empirical observations.

Curry et al. (1995) identified the “hyper” water vapor feedback in which the relative humidity (RH) is controlled by the dehydration of ice crystals, and RH against ice crystals remains approximately constant in the Arctic lower troposphere during winter, thereby increasing RH against liquid water as temperature increases. This RH increase, in turn, acts as positive feedback through the water vapor spectral “window” under an extremely dry environment. Michibata (2024) also argues that including the radiative effect of precipitating water droplets enhances AA. This effect was poorly explored in the past. These studies suggest that the feedback is coupled through the water vapor-cloud-precipitation conversion process.

In contrast to cloud condensation nuclei (CCN), ice-nucleating particles (INP) are not always abundant. The INP species are diverse, and their availability is poorly understood (Barr et al. 2023, Burrows et al. 2022). The availability, on the other hand, affects the mixed-phase cloud response and thus the strength of cloud phase feedback, as explained by Murray et al. (2021) and Matsui et al. (2024). Of particular importance at high-latitude sources is glacial dust, but recent studies report the importance of not only mineral but also biogenic compositions and show that the number of INPs in the Arctic atmosphere is increasing in Svalbard (Tobo et al. 2019, 2024).

Aerosols also affect the snow albedo at the surface. The surface albedo changes with snow cover, metamorphism of snow grains, and light-absorbing impurities in the snow (Warren and Wiscombe 1980, Wiscombe and Warren 1980). Observational knowledge and modeling capability of snow impurities such as dust and black carbon are steadily advancing (Bond et al. 2013, Skiles et al. 2018). However, simulating the emission and transport from remote sources is a challenge because they are affected by forest fires, ARs, and many other factors. It is worth noting that a recent global land surface model incorporates the capability of simulating the biological influence on snow albedo through the blooming of snow algae (Onuma et al. 2022).

Aerosol forcing is partially responsible for the decline of Arctic warming after the early 20th century (Aizawa et al. 2022). Wu et al. (2024) showed that aerosols have higher AA efficacy (Arctic cooling amplification) than greenhouse gases (GHGs) (Arctic warming amplification). Single-forcing experiments are useful for such attributions.

2.4 Interactions with lower latitudes

2.4.1 Role of atmospheric transport

a. Observed changes and data analysis

The role of AHT in AA has been extensively investigated. AHT is composed of dry static, latent, and kinetic energy components, the kinetic energy of which is usually neglected. Dry static energy comprises sensible heat (enthalpy) and potential energy. A recent study pointed out the contribution of the ‘dry’ component, more specifically horizontal temperature advection, to the observed trend of Arctic warming in winter from 1990 to 2016 (Clark et al. 2021).

The role of water vapor transport in warming the Arctic has attracted considerable attention at daily to climate-change time scales (e.g., Liang et al. 2023; Park et al. 2015a; Park et al. 2015b; Rydsaa et al. 2021; Woods and Caballero 2016; Woods et al. 2013; Yamanouchi 2019; Zhong et al. 2018; Zhang et al. 2023). Based on statistical analyses, Graversen and Burtu (2016) suggest that the ‘wet’ component of AHT is more effective in warming the Arctic than the dry component of AHT. The latent heat or water vapor transport not only warms the Arctic through the condensation heating, but also through the downwelling longwave radiation from water vapor or clouds (Fig. 4). Since these factors are considered more effective in warming the Arctic than the dry component, it has been suggested that AHT may not be a good indicator of the overall role of atmospheric transport. Sang et al. (2021) showed that the poleward water vapor transport at northern high latitudes increased from 1981-1998 to 1999-2016, in which the stationary eddy component was responsible for the increase, overwhelming a decrease due to the transient eddy component.

b. Modeling approach

Hwang and Frierson (2010) showed that models with larger poleward AHT at high latitudes (70ºN) tend to exhibit smaller AA in CMIP3 models. This relation may result from the reduction in the poleward transport of dry static energy due to a decrease in the meridional temperature gradient accompanied by AA. Stuecker et al. (2018) demonstrated that, in their model, AA is primarily driven by the locally induced lapse-rate feedback, triggered by the zonally banded CO_2 forcing, but they also noted a significant contribution to Arctic warming from AHT. Hori and Yoshimori (2023) showed that the effect of anomalous winter horizontal temperature advection would change from warming to cooling in winter as global warming progresses in the future, and that this shift arises because of competition between large-scale atmospheric circulation and transient eddy components.

The notion of higher efficacy of the wet component compared to the dry component in warming the Arctic surface was supported by Yoshimori et al. (2017), who employed both numerical experiments and feedback analysis to investigate the role of AHT changes. Other modeling studies also stress the important role of water vapor transport (e.g., Hwang et al. 2011; Woods et al. 2017). Based on the large ensemble simulations, the observed upward trend of AR frequency impeding the winter sea ice growth in the Barents-Kara Sea introduced in Section 2.2 was attributed to external forcing as well as internal variability originating in the tropics (Zhang et al. 2023). Hori et al. (2024) argue that the efficacy of winter poleward water vapor transport from lower latitudes in moistening the Arctic diminishes as global warming progresses in the future because the meridional specific humidity gradient decreases with the enhanced evaporation from the ice-retreated open water in the Arctic.

2.4.2 Role of ocean transport

a. Observed changes and data analysis

The Arctic Ocean is connected to mid-latitude oceans via four passages; the Barents Sea Opening (BSO), the Bering Strait, the Fram Strait, and the Davis Strait (Beszczynska-Möller et al. 2011)[3]. The annual mean OHT through each passage is estimated to be 73, 14±5, 36±6, and 20±9 terawatts (TW), respectively (Docquier et al. 2021). The total amount of OHT is estimated to be approximately 16% of its atmospheric counterpart (Mayer et al. 2019). Nevertheless, the relative roles of the OHT and AHT dynamics in Arctic warming are poorly understood. Eldevik et al. (2012) referred to the expansion of ice-free region where no freezing occurs during winter in the Barents Sea as “Atlantification”, and attributed it to a positive trend in OHT through the BSO. A warming trend of the Atlantic Water inflow to the Arctic Ocean through the Fram Strait was also reported by Beszczynska-Möller et al. (2012). However, determining the relative contribution of oceanic advection and atmospheric forcing appears to be complex (Asbjørnsen et al. 2020). Polyakov et al. (2017) documented the expansion of “Atlantification”, a process previously observed in the western Nansen/Eurasian Basin, to the eastern Eurasian Basin. They noted that this expansion was associated with weakening of the halocline, shoaling of the intermediate-depth Atlantic water layer, and a reduction in winter ice formation. The diminished stratification implies a larger influence of warm, salty Atlantic Water on the cold and fresh surface waters in contact with

---

[3] Rudels and Carmack (2022) and Woodgate (2013) provided comprehensive overviews of the fundamental structure of water masses and their circulation in the Arctic Ocean. In addition, Carmack et al. (2015) and Timmermans and Marshall (2020) presented detailed examinations of pertinent physical processes in the Arctic Ocean.

sea ice, facilitated by increased upward fluxes (Polyakov et al. 2018; Polyakov et al. 2019; Polyakov et al. 2020a; Polyakov et al. 2020c). Despite constraints imposed by limited historical data, recent studies have observed positive trends in volume transport, and the inflow of heat and freshwater into the Arctic through the Bering Strait (Danielson et al. 2020; Peralta-Ferriz and Woodgate 2023; Woodgate 2018). In addition, an increase in heat content in the Beaufort Gyre region was attributed to the increase in inflows of Pacific Water (Polyakov et al. 2020b). Therefore, these observations underscore the increasing influence of sub-Arctic seas on the Arctic Ocean, though these processes vary by region (Ingvaldsen et al. 2021). However, the relative contribution of atmospheric forcing remains poorly understood, and the degree to which oceanic changes affect SAT increases is currently unresolved.

b. Modeling approach

By analyzing CMIP2 models, Holland and Bitz (2003) demonstrated that projections of greater AA are associated with models depicting thinner present-day sea ice and models predicting a larger future increase in poleward OHT. These relationships were further corroborated by examining CMIP3 models, with Mahlstein and Knutti (2011) confirming the former and Hwang and Frierson (2010) confirming the latter. We note that most of the models in these studies project an increase in poleward OHT at high latitudes (~70ºN) in the future. Furthermore, Mahlstein and Knutti (2011) identified a positive correlation between the simulated present-day poleward OHT and anticipated future Arctic warming. However, these studies did not distinguish between the causative factors from the observed correlations, despite their physical plausibility being acknowledged. While warming near the ocean surface can directly lead to the basal melting of sea ice, the ability of a transported heat anomaly at depth to permeate the surface through the Arctic halocline presents a complex challenge. Consequently, the comprehensive effect of changes in OHT on Arctic climate dynamics cannot be fully assessed merely by examining column-integrated energy transport.

The warming of the Arctic Ocean is attributed to an augmented poleward OHT in certain models and to net surface heat flux in others among CMIP5 models (Burgard and Notz 2017). On the contrary, in their analysis of CMIP6 models, Shu et al. (2022) found that while enhanced poleward OHT contributes to an increase in the heat content of the Arctic Ocean in all models. This effect is partially mitigated by the increase in heat released to the atmosphere, contributing to a warming of the overlying atmosphere. A consistent increase in high-latitude OHT associated with warming across a range of GHG-forcing has also been reported (Koenigk and Brodeau 2017; van der Linden et al. 2019).

Nummelin et al. (2017) attributed the increase in poleward OHT in CMIP5 models to a reduction in heat release from the subpolar ocean to the atmosphere before flowing into the Arctic. The effect of a weakening of Atlantic meridional overturning circulation (AMOC) on high-latitude OHT varies over time, primarily because of the interplay in the subpolar ocean between the reduced surface heat loss and the lower heat influx from more temperate regions (Garuba et al. 2020; Lee et al. 2024). Using single-model large ensemble simulations, Årthun et al. (2019) observed that changes in local atmospheric circulation lead to a reduction in volume transport through the BSO. In CMIP6 models, the increases in poleward OHT through both the BSO and Bering Strait primarily result from temperature rather than velocity changes (Shu et al. 2022). Bitz et al. (2006) also showed that a decrease in surface albedo over the Arctic Ocean can enhance poleward OHT, and Dai (2022) even argues that AA is the cause of AMOC weakening rather than its consequence. Haine et al. (2023), Lee et al. (2024), and Pontes and Menviel (2024) studied the impact of Arctic freshening on the AMOC. A further complication arises because the interpretation of climatological OHT and its variations are sensitive to model resolution (Decuypère et al. 2022; Docquier et al. 2019; Heuzé and Årthun 2019), which will be touched upon again in Section 4.3. In addition, CMIP6 models generally suffer from cold biases over the Greenland Sea, the Barents Sea, and the Kara Sea, which appear to be related to the Atlantic OHT at 70ºN and the area of sea ice (Cai et al. 2021). The causality and mechanisms underlying the increase in poleward OHT under conditions of global and Arctic warming remain critical yet unresolved inquiries (Saenko et al. 2024).

Based on a simple theoretical model, Aylmer et al. (2020) proposed that the changes in OHT are about twice as effective as the changes in AHT in driving the retreat of sea ice edges. The role of OHT as a primary driver of sea ice edges and sea ice cover over the continental shelf was also suggested by Aylmer et al. (2022) and Auclair and Tremblay

(2018), respectively. In the deeper regions of the Arctic beyond the marginal ice zone, where the direct influence of changes in OHT are less pronounced, the role of atmospheric forcing may become more important (Auclair and Tremblay 2018; Aylmer et al. 2022; Singh et al. 2017). Docquier et al. (2021) attempted to highlight the effect of changes in OHT in Arctic sea-ice loss by nudging SST in the North Atlantic and North Pacific regions to higher values, but these experiments did not entirely isolate the atmospheric contribution to Arctic warming. Readers are referred to Docquier and Koenigk (2021) for a comprehensive review of the relationship between OHT and Arctic sea-ice dynamics.

It is suggested that ocean surface warming in the Gulf Stream region profoundly impacts the Barents Sea ice through the atmospheric Rossby waves (Sato et al. 2014) and the ocean heat transport (Yamagami et al. 2022). As the Gulf Stream and Kuroshio have a covarying component (Kohyama et al. 2021), the hemispheric connection between the western boundary currents and the Arctic may deserve future study.

2.4.3 Impact on the mid-latitude atmospheric circulation and potential feedback to AA

The consequences of AA are not limited to the Arctic but may have profound impacts outside the Arctic. Much discussion has been made on the influence of the Barents-Kara Sea ice loss on the mid-latitude climate, particularly the cooling signature in the Eurasian continent during winter and the westerly jet changes (Cohen et al. 2014, Smith et al. 2022). Although important, the influence of AA on middle latitude is not the focus of this article, and only an overview is provided here.

While there is a wealth of literature, no quantitative conclusion has been reached (Blackport and Screen 2020, Cohen et al. 2023, Cohen et al. 2020, Screen et al. 2018b). Some of the controversies are related to the problem setting itself (Barnes and Screen 2015, Outten et al. 2023), disagreement among analyses and/or models (Blackport et al. 2019, Dai and Song 2020, Mori et al. 2014, Nakamura et al. 2015), underestimation of both IV and EX components in numerical models (Mori et al. 2019), model bias in the background climate state (Sigmond and Sun 2024) and consideration of stratospheric processes (Hanna et al. 2024, Nakamura et al. 2016). The emergent, simplified qualitative picture is that the mid-latitude jet tends to shift poleward due to the increase of meridional temperature gradient in the upper troposphere and equatorward due to the decrease in the lower troposphere. The resultant response is determined by the ‘tag-of-war’ between these two contributions (Deser et al. 2015, Hay et al. 2022, Screen et al. 2018a) through the thermal wind balance and the feedback by eddies (Smith et al. 2022).

The increasing meandering of mid-latitude jets was also suggested (Francis and Vavrus 2012). The change in ‘waviness’, however, depends on the metric used (Geen et al. 2023), and the theory for the mechanism of jet meandering remains to be established.

It is worth noting that the response of the atmospheric circulation to AA may feedback to AA positively (Nakamura et al., 2015). In particular, the meridional displacement or meandering of jets and the shift of storm tracks may also feedback to AA through the occurrence of extreme events and associated warm and moist air advection. Therefore, more attention needs to be paid to the bidirectional 'communication' between high and mid-latitudes in future studies.

3. **Paleoclimate perspective**

3.1 Relevance, aim, and scope

Paleoclimate archive provides information about climate states and variabilities that the Earth has undergone beyond the range of instrumental observations. Paleoclimate modeling, on the other hand, offers a unique opportunity to evaluate numerical models based on such records from the real world as well as to study the physical mechanism of how the climate system responds to the large external forcing (Braconnot et al. 2012; Joussaume and Taylor 1995).

In this section, we focus on the three extensively studied past warm periods: the mid-Holocene (MH), the last interglacial (LIG), and the mid-Pliocene (mPWP) (Fig. 5). These three periods are focused study targets of the Paleoclimate Modelling Intercomparison Project (PMIP4) and they are recognized for exhibiting AA, although quantitatively defining the amplification poses challenges as the global mean response can be very small (Hind et al. 2016). We are aware that the understanding of polar amplification in much older epochs, such as the Eocene, is also fundamentally important (Huber and Caballero 2011; Lunt et al. 2021; Niezgodzki et al. 2022). Nevertheless, our review is confined to the relatively recent geological epochs (i.e., MH, LIG, and mPWP), wherein the geographic conditions, such as continental configuration, do not pose an impediment in the search for a unified physical mechanism of AA across past, present, and future epochs. It is important to appreciate that such a relative role of geographic conditions was not obvious since the beginning, and it has become recognized with the community effort of data collection, experimental design, and execution of model experiments. As the future scenario forcing is dominated by the increase in GHGs, the external forcing from today in these three periods is different from what we expect for the future; particularly redistribution of insolation is predominant in the MH and LIG forcing (Sections 3.2 and 3.3). What is essentially important is, however, to connect the climate system response through the physical mechanism despite the difference in the forcing. While the accurate reconstruction of paleo-environments, with high temporal resolution, precise dating, and spatial coverage, is indispensable for paleoclimate studies, our review places greater emphasis on the modeling efforts that foster an integrated understanding of AA across different temporal contexts.

3.2 Mid-Holocene period

3.2.1 Reconstructed climate

The present interglacial period[4], the Holocene, began 11,700 years ago (ICS, 2023). The mid-Holocene was relatively warm compared to the early and late Holocene (Kaufman et al. 2020; Marcott et al. 2013; Marsicek et al. 2018; Shakun et al. 2012, but see Appendix A),

[4] The current period does not classify as an 'interglacial' in the sequence between glaciations, yet its climatic state is analogous to those observed during past interglacial intervals.

leading to references such as the ‘Holocene climatic optimum’, ‘Holocene thermal maximum’, or ‘Hypsithermal’ (Fairbridge 2009). The latest assessment by the IPCC indicates that, during the MH (6.5-5.5 kaBP[5]), the global mean temperature was 0.2–1.0ºC higher than the 1850–1900 average, with sea level differences from 1900 ranging from -3.5 to 0.5 m (Gulev et al. 2021, Fig. 2.34). Two temperature datasets, developed by Bartlein et al. (2011) and Sundqvist et al. (2010), offer valuable resources for comparative analyses with MH simulation outcomes. They were compiled primarily based on pollen and chironomid records. The site-average temperature anomaly from preindustrial (PI) at the northern high-latitude continent was 0.9 and 0.5ºC for summer and winter, respectively, with a reason for the even larger annual mean anomaly of 1.7ºC being unresolved (Sundqvist et al., 2010).

3.2.2 External forcing

The MH external forcing is summarized in Table 1. Compared to the PI baseline, the difference is predominantly attributed to the timing of the Earth’s perihelion shifting to occur around the autumnal equinox, rather than the winter solstice in the present day, coupled with a higher obliquity by approximately 0.7º. The resulting radiative forcing at northern high latitudes is characterized by an increased annual mean insolation with an enhancement in summer (Fig. 6), while global annual mean radiative forcing is negligible.

3.2.3 Modeling approach

According to the most recent CMIP6-PMIP4 model ensemble, the global mean

[5] “kaBP” stands for thousand years before present (ca. 1950).

temperature anomaly for the MH is -0.3°C relative to the PI, based on an average of 16 models (Brierley et al. 2020). Schmidt et al. (2014) reported a weak correlation between MH conditions and the CMIP5-RCP8.5 scenario for September sea ice extent anomalies from the PI period across 10 PMIP3-CMIP5 AOGCMs (Fig. 7a). Their findings suggest some relevance of MH Arctic to the future. Yoshimori and Suzuki (2019) observed that the most pronounced Arctic warming in both MH and future projections under the CMIP5-RCP4.5 scenario occurs during autumn, despite markedly different seasonal patterns in radiative forcing between the two periods. Specifically, radiative forcing in the Arctic is relatively uniform throughout the year for RCP4.5, but largely positive in summer and even negative in (modern calendar) autumn for MH. The autumnal peak in warming during the MH is attributed to astronomical insolation anomalies during summer, which facilitates sea ice melt and heat storage in the ocean mixed layer. This stored heat is subsequently released into the atmosphere from the autumn to the winter through the area of diminished sea ice cover. This mechanism of seasonal modulation of energy exchange at the sea surface is analogous to recent observations of Arctic warming, as discussed in Section 2.3.1.

Both PMIP2 and PMIP3-CMIP5 AOGCMs tend to underestimate the winter and annual mean warming at the northern high-latitude continent relative to PI (Yoshimori and Suzuki 2019; Zhang et al. 2010). Furthermore, as highlighted in Fig. 8a, the PMIP4-CMIP6 AOGCMs also tend to underestimate annual mean warming in these regions (Brierley et al. 2020, Fig. 1e).

The general trend of AOGCMs underestimating warming can potentially be resolved by incorporating biogeographical feedback mechanisms, particularly changes in vegetation cover (Chen et al. 2022; Foley et al. 1994; O'ishi and Abe-Ouchi 2011; Otto et al. 2009; Wohlfahrt et al. 2004; Wohlfahrt et al. 2008; Zhang et al. 2010). The primary mechanism for the amplification of warming involves the replacement of present-day tundra landscapes by boreal forest due to enhanced summer insolation and consequent terrestrial warming. The replacement is expected to occur on multi-decadal to a century scales if sufficient warming is achieved. This shift in vegetation cover decreases surface albedo, accelerating snow melt and subsequent sea ice reduction in the Arctic Ocean (O'ishi and Abe-Ouchi 2011). It is important to note that the warming enhanced by the dynamic vegetation feedback also peaks in autumn and winter through the seasonal modulation mechanism within the Arctic Ocean. O'ishi and Abe-Ouchi (2011) also showed that this mechanism amplifies the annual mean Arctic warming and suggest that future projections by models not incorporating the dynamic vegetation feedback result in the underestimation of the future AA (O'ishi and Abe-Ouchi 2009; O'ishi et al. 2009). The magnitude of this feedback effect is, however, model-dependent, and accurately validating simulated vegetation cover remains a challenge. Recently, Dong et al. (2022) introduced the potential influence of increased river discharge resulting from land heating on Arctic sea-ice melt during the MH, due to anomalous summer insolation. The quantitative impact of this phenomenon, however, remains an open question.

3.3 Last interglacial period

3.3.1 Reconstructed climate

The exact definition of the LIG period varies in the literature. For the purposes of this discussion, we follow IPCC-AR6 and adopt the interval from 129,000 to 116,000 years ago (IPCC-AR6 2021, Cross-Chapter Box 2.1). The LIG is recognized for being considerably warmer than the PI era, with temperature increases reaching up to +2ºC at the peak (Cline et al. 2017; McKay et al. 2011; Turney and Jones 2010; Turney et al. 2020), and a sea level rise that exceeded current levels by 5–10 m (Gulev et al. 2021, Fig. 2.34). In early studies, large-scale temperature reconstructions were aggregated by aligning the periods of peak warmth indicated by proxy records from different locations (CAPE 2006; Turney and Jones 2010). These reconstructions suggest as much as 4-6ºC and 10ºC warming for summer and annual mean, respectively, at the northern high-latitude continent. However, subsequent climate modeling studies showed that such peak warming did not occur at the same time worldwide, suggesting that the assumption of synchroneity could introduce errors in model evaluation if compared against these aggregated reconstructions (Bakker and Renssen 2014; Bakker et al. 2013). Given the challenges associated with precise chronology for this period, recent studies have attempted to compile proxy data based on absolute dating techniques, rather than inferring periods of peak warmth during the LIG period (Capron et al. 2017; Capron et al. 2014; Hoffman et al. 2017). Although the spatial coverage is far from sufficient and proxies are limited to marine records, they offer a more robust framework for assessing the accuracy of climate model outputs.

While Polyak et al. (2010) presented a case for potentially ice-free summer conditions in the central Arctic during the LIG period, Kageyama et al. (2021) provided evidence suggesting the presence of sea ice at 79ºN based on ice-sensitive biomarkers. A recent reconstruction based on microfossil abundances in marine sediment cores, including those from the central Arctic Ocean, supports the notion of a seasonally ice-free Arctic Ocean during the LIG period (Vermassen et al. 2023).

3.3.2 External forcing

The LIG external forcing is summarized in Table 1. Compared to the PI baseline, the difference is predominantly attributed to the timing of the Earth's perihelion shifting to occur around the summer solstice, coupled with a higher obliquity by approximately 0.6º. The increased eccentricity amplified the effect of perihelion shift. The resulting radiative forcing at northern high latitudes is characterized by an increased annual mean insolation with a substantial enhancement in summer (Fig. 6). This summer insolation anomaly is significantly larger than MH (Fig. 6).

3.3.3 Modeling approach

Climate model simulations have shown reasonable concordance with the CAPE project's reconstructions, indicating a 4–5ºC increase in summer Arctic temperatures (Otto-Bliesner et al. 2006). However, as highlighted in Fig.8b, subsequent studies have shown that models tend to underestimate annual mean Arctic warming (Lunt et al. 2013; Otto-Bliesner et al. 2013). For the first time, the PMIP4 organized a multi-model experiment focused on the LIG period (127 kaBP) under a common experimental framework (Otto-Bliesner et al. 2017). Across the 17 models used in this experiment, there was notable variability in the annual mean temperature response at northern high latitudes, as well as changes to sea ice area in the NH throughout the year (Otto-Bliesner et al. 2021). As in previous studies, the models generally showed that Arctic warming is more pronounced in winter (Otto-Bliesner et al. 2021; Sicard et al. 2022; Williams et al. 2020), though not for all models (Zhang et al. 2021a). O'ishi et al. (2021) and Sicard et al. (2022) reported that the excess absorption of anomalous LIG summer insolation and subsequent heat transfer from the ocean to the atmosphere are critical factors affecting the Arctic's response, with peak warming occurring in autumn as deduced based on surface energy balance analyses. The reduction in sea ice cover significantly influences air-sea heat exchange, and the observed warming is further enhanced by the cloud greenhouse effect. These mechanisms, including the seasonal modulation mechanism, are similar to those observed in both future and MH experiments, underscoring a consistent framework for understanding AA across different temporal scales (Laîné et al. 2016; Yoshimori and Suzuki 2019).

O'ishi et al. (2021) demonstrated how the amplifying warming effect, facilitated through a specific climatic mechanism, is enhanced by biogeographical vegetation feedback (Fig. 9). The northward expansion of boreal forest to the present-day tundra-covered area has been observed and recognized for some time. Their climate model, which includes a dynamic vegetation component, successfully captured this qualitative transition. A critical factor in the process is the earlier melting of snow in spring, followed by the expansion of forests, highlighting the importance of accurately modeling the accumulation of land snow, its interactions with vegetation, and the resultant albedo effects. The dynamical mechanisms underlying how warming over NH high-latitude continents induces sea ice reduction are still poorly understood, however.

Arctic sea ice cover was investigated in detail by Kageyama et al. (2021). Their findings showed that the average outcome across 16 models indicated that the seasonal minimum sea ice area was approximately half that observed in the PI simulations, while the seasonal maximum changes only slightly. When juxtaposed against proxy reconstruction, the comparison tended to be more descriptive, with some models either underestimating or overestimating sea ice area. Interestingly, the simulated sea ice area during the LIG period is correlated with the outcomes from simulations under a 1% compound annual increase of atmospheric CO_2 concentration (a standard scenario for nominal warming), but not with PI sea ice area (Fig. 7b). This finding suggests that there may be common physical mechanisms that underpin this emergent relationship, and that sea ice extent in the future may be constrained by the LIG sea ice area, provided that it is reconstructed accurately from proxies.

Diamond et al. (2021) and Guarino et al. (2020) reported that models incorporating explicit melt-pond schemes on sea ice components predicted the minimal summer sea ice extent. In particular, one model shows a sea-ice-free Arctic in summer, which would have important implications for future projections of climate change. However, the equilibrium climate sensitivities of these two models are relatively high among CMIP6 models, and higher than the 66% range of 2.6–3.9ºC and 2.5–4.0ºC estimated by Sherwood et al. (2020) and Forster et al. (2021), respectively. Utilizing the relationship between summer SAT and sea ice area as delineated by the PMIP4 models, Sime et al. (2023) propose the existence of a near sea-ice-free summer Arctic condition at 127 kaBP. Further investigations are warranted to improve reconstruction of LIG sea ice conditions, represent melt pond processes in models, and assess equilibrium climate sensitivity.

The findings of the LIG studies suggest that the albedo feedback, particularly those associated with sea-ice melt ponds and vegetation feedback, is very important for future investigation.

3.4 Mid-Pliocene period

3.4.1 Reconstructed climate

During the Cenozoic era, the Earth experienced sustained cooling globally, occasionally punctuated by well-defined warm events. The Pliocene epoch, which spanned from 5.333 to 2.58 Ma (ICS, 2023), preceded the onset of the Quaternary glacial-interglacial cycles (Fig. 5). This epoch witnessed the initial expansion of sea ice from the central Arctic Ocean for the first time at around 4 Ma, culminating in the establishment of the modern winter sea ice extent by the end of Pliocene (Knies et al. 2014). The global climate reconstruction of the mid-Pliocene period has been established by continuous efforts through the Pliocene

Research Interpretation and Synoptic Mapping (PRISM) projects (e.g., Dowsett et al. 2016). The latest assessment by the IPCC indicates that during the mid-Pliocene or mid-Piacenzian warm period (mPWP: 3.264 to 3.024 MaBP[6]), the global mean SAT was 2.5–4.0°C higher than the 1850–1900 average, and that the sea level was 5-25 m higher than that in 1900 (Gulev et al. 2021, Fig. 2.34).

From the SST reconstruction, the amplified warming at higher latitudes is globally discernible, but it is much more prominent in the northern North Atlantic Ocean where as much as 8°C warming is observed (Dowsett et al. 2012, Fig. 2; Dowsett et al. 2016, Fig. 8; Haywood et al. 2010, Fig. 7).

3.4.2 External forcing

The mPWP external forcing is summarized in Table 1. In contrast to the MH and the LIG, in which the dominant external forcings had an astronomical origin, the warmth of the mPWP is primarily attributed to higher atmospheric CO_2 levels. However, precise CO_2 values during this period are unknown because continuous ice core records only extend to 800 kaBP. Similarly, the concentrations of other trace gases (CH_4 and N_2O) are poorly known (Hopcroft et al. 2020). Furthermore, the difference in paleogeographic conditions such as oceanic gateways and orography from the modern period needs to be considered. In particular, the Greenland ice sheet is considered substantially smaller (~25% of the contemporary area), and the West Antarctic ice sheet is considered disappeared (Dowsett et al. 2016). In addition,

[6] MaBP stands for a million years before the present (ca. 1950).

the Bering Strait and channels in the Canadian Arctic Archipelago are considered closed (Dowsett et al. 2016).

3.4.3 Modeling approach

After some early modeling studies, a coordinated modeling activity, the Pliocene Model Intercomparison Project (PlioMIP), was launched in 2008 (Haywood et al. 2021). During the past two phases of PlioMIP (PlioMIP1 and PlioMIP2), the project has facilitated comprehensive comparisons between models and between model outputs and paleoenvironmental data following the coordinated experimental protocol (Haywood et al. 2011; Haywood et al. 2010; Haywood et al. 2016). The most recent project (PlioMIP2), which employs the boundary conditions provided by PRISM4, focuses on simulating marine isotope stage KM5c (3.205 MaBP), when the astronomical conditions were similar to those of the current epoch (Dowsett et al. 2016; Haywood et al. 2016). Remarkably, the ensemble mean of simulated global mean SAT differences from the PI baseline, assuming a CO_2 concentration of 400 ppm, yielded a rise of 3.2°C across 16 models in PlioMIP2. Although this result is in agreement with the IPCC assessment cited above, the model spread ranged from 1.7 to 5.2°C, which is large (Haywood et al. 2020).

While both PlioMIP1 and PlioMIP2 model simlations captured amplified Arctic warming, they tend to underestimate annual mean terrestrial warming at northern high latitudes compared to what is suggested by proxy data (de Nooijer et al. 2020; Salzmann et al. 2013). In the 16-PlioMIP2 model ensemble mean, simulated Arctic warming is 2.3 times larger than the global average, and the sea ice extent decreases by 53%. The evaluation of simulated sea ice cover is challenging as proxies are available at only three locations (de Nooijer et al. 2020). Tindall et al. (2022) investigated the discrepancies between simulations and proxy reconstruction at northern high latitudes. Their findings showed that most mismatches occur in winter, while terrestrial summer temperatures showed good alignment. They attributed this “warm winter paradox” to several factors, including deficiencies in the models, potential insensitivities of proxies to winter temperatures, and reconstruction methods that may presuppose modern analogues for the relationship between biological proxies and their environments. Lunt et al. (2009) and Lunt et al. (2012) performed the factor analysis employing numerical experiments with different sets of boundary conditions. Their findings showed that changes in orography play a significant role in the warming observed at northern high latitudes. Based on an energy balance analysis at the top of the atmosphere, Hill et al. (2014) highlighted the crucial role of surface albedo effects, driven by both prescribed changes in ice-sheet and vegetation boundary conditions, as well as simulated snow and sea ice changes. However, Tindall et al. (2022) suggested that merely refining boundary conditions is unlikely to resolve the warm winter paradox. Interestingly, as in MH and LIG, the mechanism of seasonal modulation played a central role in shaping the Arctic warming dynamics in the mPWP (Zheng et al. 2019).

The discrepancy between modelled SSTs and proxy data, which was particularly evident in the North Atlantic, has been a long-standing issue (Chan et al. 2011; Dowsett et al. 2009;

Dowsett et al. 2012). One explanation proposed for the enhanced warming in the North Atlantic involved strengthening AMOC (Raymo et al. 1996). However, Zhang et al. (2013) challenged this hypothesis based on analyses of 8 PlioMIP1 model simulations, as well as proposing that the influence of the AMOC was insufficient to explain North Atlantic warming. On the other hand, in PlioMIP2, a consensus emerged from all 15 models simulations suggesting a stronger AMOC compared to the PI era due to the closure of the Bering Strait (Chan and Abe-Ouchi 2020; Zhang et al. 2021b). Further, these models showed general alignment with SST proxy data (Fig. 10), including those pertaining to the North Atlantic (McClymont et al. 2020). Despite the simulation of a stronger AMOC, no consistent changes were seen in the depth of the overturning cell or the total northward OHT in the Atlantic (Zhang et al. 2021b). Weiffenbach et al. (2023) elucidated that while changes in the AMOC align with the overturning component of OHT alterations, the net variations in OHT emerge from the extent to which these are offset by changes in the gyre component. Additionally, Song et al. (2018) proposed that improvements in reducing model biases in contemporary simulations may also have contributed to mitigating model-data discrepancies for North Atlantic SSTs during the mPWP.

4. Discussion

4.1 Continuous observations and attribution of the changes

As summarized in Section 2.1, continuous observation records provide a foundation for our recognition of Arctic climate change. There, efforts in long-term monitoring and climate data homogenization are critical. The datasets assimilated with observations have been playing a key role in revealing the large-scale changes in the atmosphere, ocean, and sea ice conditions and the mechanism of those changes. Nevertheless, the accuracy must always be verified with direct observations. As discussed in Section 2.2, observed changes contain both EX and IV components. While a large ensemble model simulation appears to be a promising approach, further sophistication of the decomposition method may be necessary at various time scales. Specifically, there is no guarantee that models accurately simulate the magnitude of externally forced response. If done properly, the isolated EX component would be naturally connected to a century or longer future projections and the quasi-equilibrium responses recorded in paleoclimate archives. We note that the IV component may be modulated by the external forcing, and both components may not be independent.

4.2 Paleoclimate reconstruction and model evaluation

As summarized in Sections 3.2.1, 3.3.1, and 3.4.1, paleoclimate reconstructions provide a foundation for our knowledge of the climate state in the Earth's distant past. For the assessment of model performance in simulating the EX response, compilations of well-dated, seasonally resolved temperature and sea ice proxies are requested. There, paleo-data assimilation might cast new light.

The relevance of sea ice response at LIG to future projections has been pointed out. As discussed in Section 3.3.3, the LIG simulations suggest the importance of melt-pond formation and associated changes in albedo. In paleoclimate simulations, including MH and LIG periods, it has been shown that the change in vegetation distribution contributes significantly to the Arctic warming. It is of great concern, therefore, that these important feedbacks are often missing or poorly represented in models used for future projections. Other factors, such as climate sensitivity and Arctic cloud feedback, require sustained attention.

The stronger AMOC in the mPWP simulations implies that the role of AMOC may differ from that expected under a future warming scenario. This aspect needs to be carefully considered when the mPWP is viewed as an analogy for the future. Examining Arctic warming in conjunction with changes in the AMOC within the context of paleoclimate offers valuable insights for an integrated understanding of climate dynamics. Given a large uncertainty in the atmospheric CO_2 concentration for this period, model performance in simulating the mPWP Arctic warming must be assessed globally.

4.3 The effect of model bias and resolution

In climate simulations, the way models respond to external forcing is frequently affected by inaccuracies in representing extant reference conditions. The significance of minimizing these model biases should not be underestimated (Hu et al. 2017). For example, sea ice concentration can be constrained by observations, but sea ice thickness is not precisely known. The bias in initial ice thickness could introduce a bias in the simulated ice concentration change in response to external forcing because a decrease in sea ice mass determined by the energy available for melting is a product of concentration (area) and thickness. While the model resolution does not resolve all of the issues related to bias, it is one of the most important limitations and improvements can have a marked effect of model performance (Kawasaki and Hasumi 2016; Michel et al. 2023). This point is particularly relevant for ocean simulations, where the Rossby radius of deformation in the Arctic Ocean is considerably smaller than the spatial resolution of current-generation GCMs (Wang et al. 2018). The importance of ocean model resolution is visually apparent in Fig. 11 in which penetration of warm currents into the Arctic Ocean is vividly simulated in a higher resolution setting. Consequently, a hierarchy of numerical models as a research tool is required to cover all applications from paleoclimate to future climate changes. However, an integrated understanding emerges only through the constructive synthesis of insights derived from a diverse array of models.

4.4 Process-level understanding

The understanding of the Arctic warming mechanism has been built on the knowledge of individual physical processes. This holds for climate models in that they are built on numerical representations of elementary processes. The essential part of process-level understanding relies on empirical observations, including seasonal evolution of sea-ice albedo, boundary-layer structure, turbulent heat and radiative fluxes, and cloud variables (e.g., Perovich 2002; Perovich and Polashenski 2012; Tjernström et al. 2019). The most notable examples of such observations are 1997-1998 SHEBA and 2019-2020 MOSAiC programs in which the yearlong observations in the ice-covered central Arctic have enabled to measure and scrutinize various atmosphere, ocean, and sea ice variables (Nicolaus et al. 2022; Rabe et al. 2022; Shupe et al. 2022; Uttal et al. 2002). While the review of individual measurements is beyond the scope of this paper, these efforts and contributions to the discipline cannot be overstated. The short-term in-situ observations also provide valuable insight into the understanding of phenomena, as exemplified in Section 2.2 (e.g., Kodaira et al. 2020; Yamanouchi 2021).

Our review concerns that observational datasets for the surface inversion layer are spatially limited over the Arctic Ocean except for those by SHEBA and MOSAiC programs, and processes affecting its strength and vertical extent are poorly understood. Consequently, the response of lower tropospheric stratification to external forcing remains quantitatively ambiguous. Furthermore, cloud microphysics, particularly processes related to phase changes, as well as cloud dynamics present additional challenges. For example, the competing effect of shortwave and longwave radiation components associated with cloud phase change is qualitatively uncertain.

Integrating the insight from in-situ observations with large eddy simulations, single-column models, and regional modeling may be a promising step to connect them with a more large-scale perspective (e.g., Klein et al. 2009; Morrison et al. 2009, 2011b; Ovchinnikov et al. 2017; Pithan et al. 2014; Sedlar et al. 2020 and references therein; Stevens et al. 2018), as also discussed in Section 4.2 of Shupe et al. (2022).

4.5 System understanding

The cause and effect of changes in AHT and Arctic warming need to be elaborated while considering the time scale of phenomena into account. Suppose that the retreat of sea ice was caused by the increased AHT from lower latitudes. If the subsequent release of heat from the ocean to the atmosphere causes a weakening of poleward AHT by more than its initial increase, then the net poleward AHT anomaly in the time average becomes negative. In such a case, the seasonally averaged energy budget analysis would imply that the ocean drives atmospheric warming and that horizontal temperature advection in the atmosphere suppresses warming. While this interpretation is statistically sound, it distorts the sequence of physical processes, and hence the causality.

Regardless of whether temperature or moisture advection is important, the climatological interpretation must be made based on connecting the effect of weather events. It is important to quantify the extent of moisture intrusion associated with events such as ARs, atmospheric blockings, extratropical cyclones, and polar lows and to assess how global climate change modulates these events and their impact, especially since a significant portion of water vapor is transported to the Arctic during these meteorological events.

The role of AHT has not been investigated sufficiently in paleoclimate simulations of the three warm periods discussed in this review. Thus, how the AHT responds to the latitudinal and seasonal redistribution of insolation and affects Arctic warming is poorly known. Its relevance to future projections remains to be explored.

Whereas the increase of poleward OHT at northern high latitudes appears to be a robust response to the rise in atmospheric CO_2 level, its mechanism is poorly understood, as discussed in Section 2.4.2. The short record length of ocean monitoring imposes a severe limitation on isolating the forced response from IV. The quantitative impact of the OHT increase on the Arctic may differ among the subsurface ocean, the ocean mixed layer, and the atmospheric boundary layer. Consequently, an in-depth understanding and numerical representation of haloclines, turbulent atmospheric and ocean mixing, and processes associated with the sea ice and freshwater budget would be critically important. Understanding the two-way interaction between the AMOC and the Arctic climate on various time scales must be established. There, the role of AMO needs to be clarified. Adopting the atmospheric framework of Barnes and Screen (2015), several important questions remain to be addressed: a) what are the specific mechanisms by which changes in OHT can significantly impact Arctic warming; b) has such a mechanism played a role in Arctic warming to date; and c) to what extent will such a mechanism impact future Arctic warming?

Elucidating the relative roles of AHT and OHT changes and how they interact with each other (e.g., Bjerkness compensation) in the modern and paleoclimate AA are fundamental subjects. Elucidating the interplay between AHT/OHT change and Arctic local feedback processes is essential to comprehend the role of AHT/OHT in AA.

Whereas it is extremely difficult, if not impossible, to obtain process-level information into the mechanisms of AA from the Earth's distant past, paleoclimate studies provide substantial evidence on the overall response of the climate system to external forcings. In both past interglacial periods and during the mPWP, ice sheets have played an important role in shaping the Arctic climate. Given the transient nature of interglacial periods, there is a need for increased efforts to examine their time-varying characteristics, including variations in the ice sheet distribution and the effect of meltwater discharges (see Appendix B). Indeed, Hirose et al. (2025) showed that the primary factor controlling the degree of Arctic warming within the past interglacials is the remnant ice sheets from the glacial period, with the insolation difference being a secondary factor. The interaction between ice sheets and Arctic climate, along with the global constraint on ice sheet volume through global mean sea level, underscores the relevance of studies on ocean thermal expansion and the past behavior of the Antarctic ice sheet. Thus, uncertainties in these components are interconnected, indicating that a hierarchical modeling should encompass not just the resolution of various temporal and spatial scales, but also the diversity of its subsystem components.

5. Summary

Continuous monitoring has provided fundamental information about the long-term Arctic changes (Section 2.1). Large ensemble model simulations offer one way of attributing the observed changes to EX and IV components (Section 2.2), an essential first step in understanding the mechanism. It remains a challenge to verify the model-based attribution empirically.

The contribution of local atmospheric feedback processes to Arctic warming has been a focal point of extensive research, and our understanding of them has advanced considerably over the last decade. Nevertheless, there is still considerable scope for further studies to clarify the interactions among feedback processes (e.g., sea ice and cloud feedbacks) and how their components should be formulated. In both modern and past climates, one common process associated with Arctic warming is the seasonal exchange of energy between the atmosphere and the ocean. The heart of this seasonally modulated amplification mechanism is oceanic heat release in winter, which may enhance warming due to (a) the nonlinearity of the radiation law, (b) strong near-surface stratification in the atmosphere, and (c) the greenhouse effect of clouds. Therefore, it is expected that understanding and improving the numerical representation of processes at every scale associated with the Arctic annual cycles would significantly contribute to a more integrated understanding of Arctic warming in the past, present, and future (Section 2.3). Observations covering the annual cycle (e.g., MOSAiC and satellites) would be vital resources to achieve this goal.

Interactions with lower latitudes are poorly understood, and the roles of atmosphere and ocean circulartion and the cause of their changes need to be firmly established (Section 2.4). This review suggests expanding the framework of understanding from unidirectional influence to bidirectional interaction between the Arctic and mid-latitudes.

The review of the MH, LIG, and mPWP studies reveals that the proxy data warns against climate models used for future projections in their ability to reproduce the winter and annual mean warming to a sufficient degree at northern high latitudes. While this does not immediately imply errors in future projections, the result of this ‘screening exam’ from independent cases should never be overlooked (Section 3).

Microscopic, individual physical processes directly identified by the in-situ observations are indirectly constrained by macroscopic responses of the climate system to external forcings (e.g., paleoclimatic observations). The hierarchical observational insight and modeling activity would connect the process-oriented bottom-up perspective and the system-oriented top-down perspective. Scientists focusing on modern climate and those on paleoclimate must work together now more than ever, and we hope this review provides knowledge to accelerate their collaborative activities.

Data Availability Statement

The HadCRUT5 data were downloaded from https://crudata.uea.ac.uk/cru/data/temperature/ for Figs. 1 and 2. The NSIDC sea ice data and Rutgers University snow data were downloaded from https://nsidc.org/data/g02135/versions/3 and https://climate.rutgers.edu/snowcover/index.php, respectively, for Fig. 2. The ERA5 reanalysis data were downloaded from https://www.ecmwf.int/en/forecasts/dataset/ecmwf-reanalysis-v5, and the ORA-S4 from https://www.cen.uni-hamburg.de/en/icdc/data/ocean/easy-init-ocean/ecmwf-ocean-reanalysis-system-4-oras4.html for Fig. 3. Estimated global mean surface temperature anomaly over the past 5 million years are downloaded from https://dx.doi.org/10.5285/0f05c2fb8f814d60ac2d657a70e9a7f5 for Fig. 5. The CMIP6-PMIP4 data are available from https://pcmdi.llnl.gov/CMIP6/ for Figs. 8 and 10. Surface air temperature reconstruction data for MH and LIG are taken from Table 1a of Sundqvist et al. (2010) and from Supporting Information of Turney and Jones (2010), respectively, for Fig. 8. The PRISM3 SST anomaly reconstruction data were downloaded from https://geology.er.usgs.gov/egpsc/prism/prism_1_23/prism_data.html for Fig. 10. The simulated data for Figs. 11a and 11b are available in J-STAGE Data https://doi.org/10.34474/data.jmsj.2025-027. Observation data for Fig. 11c are available from https://climate.mri-jma.go.jp/pub/ocean/ts/.

Acknowledgments

This work was supported by the Arctic Challenge for Sustainability II Program (Grant No. JPMXD1420318865) and a Grant-in-Aid from JSPS KAKENHI (Grant No. JP19H05595, JP24H00256, and JP24H02346). Valuable comments from the editor and two anonymous reviewers are appreciated. We acknowledge the Met Office Hadley Centre and the Climatic Research Unit at the University of East Anglia for providing the HadCRUT5 data, the

National Snow and Ice Data Center for the sea ice extent data, the Rutgers University Global Snow Lab for the snow cover extent data. We also acknowledge the Copernicus Climate Change Service and the European Centre for Medium-Range Weather Forecasts for providing ERA5 and ORA-S4 data. Neither the European Commission nor ECMWF is responsible for any use that may be made of the Copernicus information or data it contains. We further acknowledge the World Climate Research Programme's Working Group on Coupled Modelling, which is responsible for CMIP, and we thank the climate modeling groups (listed in Table 2 of this paper) for producing and making available their model output. For CMIP, the US Department of Energy's Program for Climate Model Diagnosis and Intercomparison provides coordinating support and led the development of the software infrastructure, in partnership with the Global Organization for Earth System Science Portals. We thank PMIP for coordinating the experiment and preparing the dataset. We also thank the developers of the freely available software, acccmip6, NCO, CDO, and NCL.

Appendix

A. Relevant and important controversy for the Holocene climate evolution

Recent studies challenge the globally warmer view in the middle of the Holocene, suggesting a more moderate climate than was previously thought (Kaufman and Broadman 2023). Disparities between climate model simulations, which show a steady global warming trend from the early to the late Holocene, and proxy-based temperature reconstructions, often referred to as the ‘Holocene temperature conundrum’ (Liu et al. 2014), have been ascribed to methodological limitations arising from inadequate spatial coverage of proxy records (Bader et al. 2020; Osman et al. 2021), seasonally biased recording of proxies (Bova et al. 2021; Erb et al. 2022; Liu et al. 2014), and/or missing or poor representation of feedback processes in numerical models, including geographical changes in vegetation and atmospheric dust loading (Liu et al. 2018; Liu et al. 2014; Thompson et al. 2022). Understanding the nuances of Arctic warming is important for an accurate grasp of global climate evolution through the Holocene (Bader et al. 2020), and thus the importance of vegetation feedback is not limited to AA but extended globally (O’ishi and Abe-Ouchi 2011; Thompson et al. 2022). It was also pointed out that the Arctic warmth during the Holocene is controlled by a remnant ice sheet from the glacial period (Hirose et al. 2025). These highlights underline the need for climate models to include transient simulations with dynamic vegetation and ice sheet components.

B. The effect of meltwater discharge for the LIG climate evolution

Meltwater discharge from ice sheets was not explicitly specified in the PMIP4 equilibrium experiment protocol, resulting in no substantial changes observed in AMOC simulations (Jiang et al. 2023). The potential effect of meltwater discharge, particularly due to shrinking of the Greenland ice sheet, has been investigated (Otto-Bliesner et al. 2006). The potential impact of AMOC weakening or strengthening, and its impact on LIG climate through changes in meridional OHT, have been explored in several studies, including Guarino et al. (2023);

Kageyama et al. (2021); Pedersen et al. (2016); Swingedouw et al. (2009). Stone et al. (2016) proposed that meltwater discharge from remnant ice sheets from the preceding glacial stage at around 130 kaBP produced a weaker AMOC, leading to cooler and warmer conditions in the North Atlantic and Southern Ocean, respectively, compared to the present day. This pattern is consistent with the bipolar seesaw phenomenon corroborated by proxy-based reconstructions (Capron et al. 2014). Similarly, Govin et al. (2012) simulated a weaker AMOC in the early LIG period, attributing it to the delayed onset of peak warming at northern high latitudes. These findings underlie the importance of accurately assessing the volume and timing of meltwater discharges during the LIG period, and the need for transient climate simulations as undertaken by Obase and Abe-Ouchi (2019) and Obase et al. (2021). Furthermore, the development and application of interactive climate-ice sheet models are strongly desired.

References

Aizawa, T., N. Oshima, and S. Yukimoto, 2022: Contributions of anthropogenic aerosol forcing and multidecadal internal variability to mid-20th century Arctic cooling-CMIP6/DAMIP multimodel analysis. *Geophys. Res. Lett.*, **49**, doi:10.1029/2021GL097093.

Aizawa, T., M. Ishii, N. Oshima, S. Yukimoto, and H. Hasumi, 2021: Arctic warming and associated sea ice reduction in the early 20th century induced by natural forcings in

MRI-ESM2.0 climate simulations and multimodel analyses. *Geophys. Res. Lett.*, **48**, doi: 10.1029/2020GL092336.

Alexeev, V. A., 2003: Sensitivity to CO_2 doubling of an atmospheric GCM coupled to an oceanic mixed layer: A linear analysis. *Clim. Dyn.*, **20,** 775-787.

Alexeev, V. A., P. L. Langen, and J. R. Bates, 2005: Polar amplification of surface warming on an aquaplanet in "ghost forcing" experiments without sea ice feedbacks. *Clim. Dyn.*, **24,** 655-666.

AMAP, 2021: AMAP Arctic Climate Change Update 2021: Key Trends and Impacts. Arctic Monitoring and Assessment Programme (AMAP), 148pp.

Årthun, M., T. Eldevik, and L. H. Smedsrud, 2019: The role of Atlantic heat transport in future Arctic winter sea ice loss. *J. Climate*, **32,** 3327-3341.

Asbjørnsen, H., M. Årthun, Ø. Skagseth, and T. Eldevik, 2020: Mechanisms underlying recent Arctic Atlantification. *Geophys. Res. Lett.*, **47**, doi:10.1029/2020GL088036.

Auclair, G., and L. B. Tremblay, 2018: The role of ocean heat transport in rapid sea ice declines in the Community Earth System Model Large Ensemble. *J. Geophys. Res.-Oceans*, **123,** 8941-8957.

Aylmer, J., D. Ferreira, and D. Feltham, 2020: Impacts of oceanic and atmospheric heat transports on sea ice extent. *J. Climate*, **33,** 7197-7215.

Aylmer, J., D. Ferreira, and D. Feltham, 2022: Different mechanisms of Arctic and Antarctic sea ice response to ocean heat transport. *Clim. Dyn.*, **59,** 315-329.

Bader, J., J. Jungclaus, N. Krivova, S. Lorenz, A. Maycock, T. Raddatz, H. Schmidt, M. Toohey, C. J. Wu, and M. Claussen, 2020: Global temperature modes shed light on the Holocene temperature conundrum. *Nat. Commun.*, **11**, 4726, doi:10.1038/s41467-020-18478-6.

Bakker, P., and H. Renssen, 2014: Last interglacial model–data mismatch of thermal maximum temperatures partially explained. *Clim. Past*, **10,** 1633-1644.

Bakker, P., E. J. Stone, S. Charbit, M. Gröger, U. Krebs-Kanzow, S. P. Ritz, V. Varma, V. Khon, D. J. Lunt, U. Mikolajewicz, M. Prange, H. Renssen, B. Schneider, and M. Schulz, 2013: Last interglacial temperature evolution – a model inter-comparison. *Clim. Past*, **9,** 605-619.

Balmaseda, M. A., K. Mogensen, and A. T. Weaver, 2013: Evaluation of the ECMWF ocean reanalysis system ORAS4. *Q. J. R. Meteorol. Soc.*, **139,** 1132-1161.

Barnes, E. A. and J. A. Screen, 2015: The impact of Arctic warming on the midlatitude jet-stream: Can it? Has it? Will it? Wiley Interdisciplinary Reviews: *Clim, Chan.*, **6**, 277-286.

Barr, S. L., B. Wyld, J. B. McQuaid, R. R. Neely, III and B.J. Murray, 2023: Southern Alaska as a source of atmospheric mineral dust and ice-nucleating particles. *Sci. Adv*., **9**, doi:10.1126/sciadv.adg3708.

Bartlein, P. J., S. P. Harrison, S. Brewer, S. Connor, B. A. S. Davis, K. Gajewski, J. Guiot, T. I. Harrison-Prentice, A. Henderson, O. Peyron, I. C. Prentice, M. Scholze, H. Seppa, B. Shuman, S. Sugita, R. S. Thompson, A. E. Viau, J. Williams, and H. Wu, 2011:

Pollen-based continental climate reconstructions at 6 and 21 ka: a global synthesis. *Clim. Dyn.*, **37,** 775-802.

Beszczynska-Möller, A., E. Fahrbach, U. Schauer, and E. Hansen, 2012: Variability in Atlantic water temperature and transport at the entrance to the Arctic Ocean, 1997-2010. *ICES Journal of Marine Science*, **69,** 852-863.

Beszczynska-Möller, A., R. A. Woodgate, C. Lee, H. Melling, and M. Karcher, 2011: A Synthesis of Exchanges Through the Main Oceanic Gateways to the Arctic Ocean. *Oceanography*, **24,** 82-99.

Bintanja, R., R. G. Graversen, and W. Hazeleger, 2011: Arctic winter warming amplified by the thermal inversion and consequent low infrared cooling to space. *Nature Geoscience*, **4,** 758-761.

Bintanja, R., E. C. van der Linden, and W. Hazeleger, 2012: Boundary layer stability and Arctic climate change: a feedback study using EC-Earth. *Clim. Dyn.*, **39,** 2659-2673.

Bitz, C. M., P. R. Gent, R. A. Woodgate, M. M. Holland, and R. Lindsay, 2006: The influence of sea ice on ocean heat uptake in response to increasing CO_2. *J. Climate*, **19,** 2437-2450.

Blackport, R. and J. A. Screen, 2020: Weakened evidence for mid-latitude impacts of Arctic warming. *Nat. Clim. Chan.*, **10**, 1065-1066.

Blackport, R., J. A. Screen, K. van der Wiel and R. Bintanja, 2019: Minimal influence of reduced Arctic sea ice on coincident cold winters in mid-latitudes. *Nat. Clim. Chan.*, **9**, 697-704.

Boeke, R. C., P. C. Taylor, and S. A. Sejas, 2021: On the Nature of the Arctic's Positive Lapse-Rate Feedback. *Geophys. Res. Lett.*, **48**, doi:10.1029/2020GL091109.

Bond, T. C. and Coauthors, 2013: Bounding the role of black carbon in the climate system: A scientific assessment. *J. Geophys. Res.*, **118**, 5380-5552.

Bony, S., R. Colman, V. M. Kattsov, R. P. Allan, C. S. Bretherton, J.-L. Dufresne, A. Hall, S. Hallegatte, M. M. Holland, W. Ingram, D. A. Randall, B. J. Soden, G. Tselioudis, and M. J. Webb, 2006: How well do we understand and evaluate climate change feedback processes? *J. Climate*, **19,** 3445-3482.

Bova, S., Y. Rosenthal, Z. Liu, S. P. Godad, and M. Yan, 2021: Seasonal origin of the thermal maxima at the Holocene and the last interglacial. *Nature*, **589,** 548-553.

Box, J. E., and Coauthors, 2021: Recent developments in Arctic climate observational indicators. AMAP Arctic Climate Change Update 2021: Key Trends and Impacts., 7-29pp.

Braconnot, P., S. P. Harrison, M. Kageyama, P. J. Bartlein, V. Masson-Delmotte, A. Abe-Ouchi, B. Otto-Bliesner, and Y. Zhao, 2012: Evaluation of climate models using palaeoclimatic data. *Nat. Clim. Chang.*, **2,** 417-424.

Brierley, C. M., A. Zhao, S. P. Harrison, P. Braconnot, C. J. R. Williams, D. J. R. Thornalley, X. Shi, J.-Y. Peterschmitt, R. Ohgaito, D. S. Kaufman, M. Kageyama, J. C. Hargreaves, M. P. Erb, J. Emile-Geay, R. D'Agostino, D. Chandan, M. Carré, P. J. Bartlein, W. Zheng,

Z. Zhang, Q. Zhang, H. Yang, E. M. Volodin, R. A. Tomas, C. Routson, W. R. Peltier, B. Otto-Bliesner, P. A. Morozova, N. P. McKay, G. Lohmann, A. N. Legrande, C. Guo, J. Cao, E. Brady, J. D. Annan, and A. Abe-Ouchi, 2020: Large-scale features and evaluation of the PMIP4-CMIP6 midHolocene simulations. *Clim. Past*, **16,** 1847-1872.

Burgard, C., and D. Notz, 2017: Drivers of Arctic Ocean warming in CMIP5 models. *Geophys. Res. Lett.*, **44,** 4263-4271.

Burrows, S.M. and Coauthors, 2022: Ice-nucleating particles that impact clouds and climate: Observational and modeling research needs. *Rev. Geophys.*, **60**, doi:10.1029/2021rg000745.

Cai, Z. Y., Q. L. You, F. Y. Wu, H. W. Chen, D. L. Chen, and J. D. Cohen, 2021: Arctic Warming Revealed by Multiple CMIP6 Models: Evaluation of Historical Simulations and Quantification of Future Projection Uncertainties. *J. Climate*, **34,** 4871-4892.

CAPE, 2006: Last Interglacial Arctic warmth confirms polar amplification of climate change. *Quat. Sci. Rev.*, **25,** 1383-1400.

Capron, E., A. Govin, R. Feng, B. L. Otto-Bliesner, and E. W. Wolff, 2017: Critical evaluation of climate syntheses to benchmark CMIP6/PMIP4 127 ka Last Interglacial simulations in the high-latitude regions. *Quat. Sci. Rev.*, **168,** 137-150.

Capron, E., A. Govin, E. J. Stone, V. Masson-Delmotte, S. Mulitza, B. Otto-Bliesner, T. L. Rasmussen, L. C. Sime, C. Waelbroeck, and E. W. Wolff, 2014: Temporal and spatial structure of multi-millennial temperature changes at high latitudes during the Last

Interglacial. *Quat. Sci. Rev.*, **103,** 116-133.

Carmack, E., I. Polyakov, L. Padman, I. Fer, E. Hunke, J. Hutchings, J. Jackson, D. Kelley, R. Kwok, C. Layton, H. Melling, D. Perovich, O. Persson, B. Ruddick, M. L. Timmermans, J. Toole, T. Ross, S. Vavrus, and P. Winsor, 2015: Toward Quantifying the Increasing Role of Oceanic Heat in Sea Ice Loss in the New Arctic. *Bull. Amer. Meteor. Soc.*, **96,** 2079-2105.

Chan, W.-L., and A. Abe-Ouchi, 2020: Pliocene Model Intercomparison Project (PlioMIP2) simulations using the Model for Interdisciplinary Research on Climate (MIROC4m). *Clim. Past*, **16,** 1523-1545.

Chan, W. L., A. Abe-Ouchi, and R. Ohgaito, 2011: Simulating the mid-Pliocene climate with the MIROC general circulation model: experimental design and initial results. *Geosci. Model Dev.*, **4,** 1035-1049.

Chen, X. D. and A. G. Dai, 2024: Quantifying Contributions of External Forcing and Internal Variability to Arctic Warming During 1900-2021. *Earths Future*, **12**, doi:10.1029/2023ef003734.

Chen, J., Q. Zhang, E. Kjellström, Z. Lu, and F. Chen, 2022: The Contribution of Vegetation-Climate Feedback and Resultant Sea Ice Loss to Amplified Arctic Warming During the Mid-Holocene. *Geophys. Res. Lett.*, **49**, doi:10.1029/2022GL098816.

Clark, J. P., V. Shenoy, S. B. Feldstein, S. Lee, and M. Goss, 2021: The Role of Horizontal Temperature Advection in Arctic Amplification. *J. Climate*, **34,** 2957-2976.

Cline, R. M. L., J. D. Hays, W. L. Prell, W. F. Ruddiman, T. C. Moore, N. G. Kipp, B. E. Molfino, G. H. Denton, T. J. Hughes, W. L. Balsam, C. A. Brunner, J.-C. Duplessy, A. G. Esmay, J. L. Fastook, J. Imbrie, L. D. Keigwin, T. B. Kellogg, A. McIntyre, R. K. Matthews, A. C. Mix, J. J. Morley, N. J. Shackleton, S. S. Streeter, and P. R. Thompson, 2017: The Last Interglacial Ocean. *Quaternary Research*, **21,** 123-224.

Cohen, J., L. Agel, M. Barlow and D. Entekhabi, 2023: No detectable trend in mid-latitude cold extremes during the recent period of Arctic amplification. *Commun. Earth Environ.*, **4**, doi:10.1038/s43247-023-01008-9.

Cohen, J. and Coauthors, 2014: Recent Arctic amplification and extreme mid-latitude weather. *Nat. Geosci.*, **7**, 627-637.

Cohen, J. and Coauthors, 2020: Divergent consensuses on Arctic amplification influence on midlatitude severe winter weather. *Nat. Clim. Chan.*, **10**, 20-29.

Comiso, J. C. and F. Nishio, 2008: Trends in the sea ice cover using enhanced and compatible AMSR-E, SSM/I, and SMMR data. *J. Geophys. Res.*, **113**, doi:10.1029/2007jc004257.

Crook, J. A., P. M. Forster, and N. Stuber, 2011: Spatial Patterns of Modeled Climate Feedback and Contributions to Temperature Response and Polar Amplification. *J. Climate*, **24,** 3575-3592.

Curry, J. A., W. B. Rossow, D. Randall and J. L. Schramm, 1996: Overview of Arctic cloud and radiation characteristics. *J. Climate*, **9**, 1731-1764.

Curry, J. A., J. L. Schramm, M. C. Serreze and E. E. Ebert, 2012: Water vapor feedback over the Arctic Ocean. *J. Geophys. Res.*, **100**, 14223-14229.

Dai, A. G., 2022: Arctic amplification is the main cause of the Atlantic meridional overturning circulation weakening under large CO_2 increases. *Clim. Dyn.*, **58,** 3243-3259.

Dai, A. G. and M. R. Song, 2020: Little influence of Arctic amplification on mid-latitude climate. *Nat. Clim. Chan.*, **10**, 231-237.

Dai, A. G., and M. T. Jenkins, 2023: Relationships among Arctic warming, sea-ice loss, stability, lapse rate feedback, and Arctic amplification. *Clim. Dyn.*, **61,** 5217-5232.

Dai, A. G., D. H. Luo, M. R. Song, and J. P. Liu, 2019: Arctic amplification is caused by sea-ice loss under increasing CO_2. *Nat. Commun.*, **10**, 121, doi: 10.1038/s41467-018-07954-9.

Danielson, S. L., O. Ahkinga, C. Ashjian, E. Basyuk, L. W. Cooper, L. Eisner, E. Farley, K. B. Iken, J. M. Grebmeier, L. Juranek, G. Khen, S. R. Jayne, T. Kikuchi, C. Ladd, K. Lu, R. M. McCabe, G. W. K. Moore, S. Nishino, F. Ozenna, R. S. Pickart, I. Polyakov, P. J. Stabeno, R. Thoman, W. J. Williams, K. Wood, and T. J. Weingartner, 2020: Manifestation and consequences of warming and altered heat fluxes over the Bering and Chukchi Sea continental shelves. *Deep-Sea Res. Part II-Topical Studies in Oceanography*, **177**, 104781, doi:10.1016/j.dsr2.2020.104781.

de Nooijer, W., Q. Zhang, Q. Li, Q. Zhang, X. Li, Z. Zhang, C. Guo, K. H. Nisancioglu, A.

M. Haywood, J. C. Tindall, S. J. Hunter, H. J. Dowsett, C. Stepanek, G. Lohmann, B. L. Otto-Bliesner, R. Feng, L. E. Sohl, M. A. Chandler, N. Tan, C. Contoux, G. Ramstein, M. L. J. Baatsen, A. S. von der Heydt, D. Chandan, W. R. Peltier, A. Abe-Ouchi, W.-L. Chan, Y. Kamae, and C. M. Brierley, 2020: Evaluation of Arctic warming in mid-Pliocene climate simulations. *Clim. Past*, **16,** 2325-2341.

Decuypère, M., L. B. Tremblay, and C. O. Dufour, 2022: Impact of Ocean Heat Transport on Arctic Sea Ice Variability in the GFDL CM2-O Model Suite. *J. Geophys. Res.: Oceans*, **127**, doi:10.1029/2021JC017762.

Deser, C., R. A. Tomas and L. T. Sun, 2015: The role of ocean-atmosphere coupling in the zonal-mean atmospheric response to Arctic sea ice loss. J. Climate, **28**, 2168-2186.

Devasthale, A., J. Sedlar, M. Tjernström, and A. Kokhanovsky, 2000: A climatological overview of Arctic clouds. In Physics and Chemistry of the Arctic Atmosphere. A. Kokhanovsky and C. Tomasi (Eds.), Springer Polar Sciences, Springer Nature Switzerland, 331-360.

Ding, Q., J. M. Wallace, D. S. Battisti, E. J. Steig, A.J . Gallant, H. J. Kim and L. Geng, 2014: Tropical forcing of the recent rapid Arctic warming in northeastern Canada and Greenland. *Nature*, **509**, 209-212.

Ding, Q. and Coauthors, 2018: Fingerprints of internal drivers of Arctic sea ice loss in observations and model simulations. *Nat. Geosci.*, **12**, 28-33.

Dörr, J.S., D.B. Bonan, M. Arthun, L. Svendsen and R.C.J. Wills, 2023: Forced and internal components of observed Arctic sea-ice changes. Cryosphere, 17, 4133-4153. 10.5194/tc-17-4133-2023.

Docquier, D., and T. Koenigk, 2021: A review of interactions between ocean heat transport and Arctic sea ice. *Environ. Res. Lett.*, **16**, doi:10.1088/1748-9326/ac30be.

Docquier, D., T. Koenigk, R. Fuentes-Franco, M. P. Karami, and Y. Ruprich-Robert, 2021: Impact of ocean heat transport on the Arctic sea-ice decline: a model study with EC-Earth3. *Clim. Dyn.*, **56,** 1407-1432.

Docquier, D., J. P. Grist, M. J. Roberts, C. D. Roberts, T. Semmler, L. Ponsoni, F. Massonnet, D. Sidorenko, D. V. Sein, D. Iovino, A. Bellucci, and T. Fichefet, 2019: Impact of model resolution on Arctic sea ice and North Atlantic Ocean heat transport. *Clim. Dyn.*, **53,** 4989-5017.

Dong, J., X. Shi, X. Gong, A. S. Astakhov, L. Hu, X. Liu, G. Yang, Y. Wang, Y. Vasilenko, S. Qiao, A. Bosin, and G. Lohmann, 2022: Enhanced Arctic sea ice melting controlled by larger heat discharge of mid-Holocene rivers. *Nat. Commun.*, **13,** 5368, doi: 10.1038/s41467-022-33106-1.

Dowsett, H., A. Dolan, D. Rowley, R. Moucha, A. M. Forte, J. X. Mitrovica, M. Pound, U. Salzmann, M. Robinson, M. Chandler, K. Foley, and A. Haywood, 2016: The PRISM4 (mid-Piacenzian) paleoenvironmental reconstruction. *Clim. Past*, **12,** 1519-1538.

Dowsett, H. J., M. A. Chandler, and M. M. Robinson, 2009: Surface temperatures of the Mid-Pliocene North Atlantic Ocean: implications for future climate. *Philos Trans A Math*

Phys Eng Sci, **367,** 69-84.

Dowsett, H. J., M. M. Robinson, D. K. Stoll, and K. M. Foley, 2010: Mid-Piacenzian mean annual sea surface temperature analysis for data-model comparisons. *Stratigraphy*, **7,** 189-198.

Dowsett, H. J., M. M. Robinson, A. M. Haywood, D. J. Hill, A. M. Dolan, D. K. Stoll, W.-L. Chan, A. Abe-Ouchi, M. A. Chandler, N. A. Rosenbloom, B. L. Otto-Bliesner, F. J. Bragg, D. J. Lunt, K. M. Foley, and C. R. Riesselman, 2012: Assessing confidence in Pliocene sea surface temperatures to evaluate predictive models. *Nat. Clim. Chang.*, **2,** 365-371.

Eldevik, T., M. Årthun, L. H. Smedsrud, Ø. Skagseth, and R. B. Ingvaldsen, 2012: Quantifying the Influence of Atlantic Heat on Barents Sea Ice Variability and Retreat. *J. Climate*, **25,** 4736-4743.

England, M., A. Jahn, and L. Polvani, 2019: Nonuniform Contribution of Internal Variability to Recent Arctic Sea Ice Loss. *J. Climate*, **32,** 4039-4053.

Estilow, T. W., A. H. Young and D. A. Robinson, 2015: A long-term Northern Hemisphere snow cover extent data record for climate studies and monitoring. *Earth Sys. Sci. Data*, **7**, 137-142.

Erb, M. P., N. P. McKay, N. Steiger, S. Dee, C. Hancock, R. F. Ivanovic, L. J. Gregoire, and P. Valdes, 2022: Reconstructing Holocene temperatures in time and space using paleoclimate data assimilation. *Clim. Past*, **18,** 2599-2629.

Fairbridge, R. W., 2009: Hypsithermal. *Encyclopedia of Paleoclimatology and Ancient*

Environments, V. Gornitz, Ed., Springer Netherlands, 451-452.

Feldl, N., S. Po-Chedley, H. K. A. Singh, S. Hay, and P. J. Kushner, 2020: Sea ice and atmospheric circulation shape the high-latitude lapse rate feedback. *Npj Climate and Atmospheric Science*, **3**, doi:10.1038/s41612-020-00146-7.

Foley, J. A., J. E. Kutzbach, M. T. Coe, and S. Levis, 1994: Feedbacks between climate and boreal forests during the Holocene epoch. *Nature*, **371,** 52-54.

Forster, P., T. Storelvmo, K. Armour, W. Collins, J.-L. Dufresne, D. Frame, D. J. Lunt, T. Mauritsen, M. D. Palmer, M. Watanabe, M. Wild, and H. Zhang, 2021: The Earth's Energy Budget, Climate Feedbacks, and Climate Sensitivity. *Climate Change 2021: The Physical Science Basis. Contribution of Working Group I to the Sixth Assessment Report of the Intergovernmental Panel on Climate Change.*, V. Masson-Delmotte, and Coauthors, Eds., Cambridge University Press, 923-1054.

Francis, J. A. and S. J. Vavrus, 2012: Evidence linking Arctic amplification to extreme weather in mid-latitudes. *Geophys. Res. Lett.*, **39**, L06801, doi:10.1029/2012gl051000.

Garuba, O. A., H. A. Singh, E. Hunke, and P. J. Rasch, 2020: Disentangling the Coupled Atmosphere-Ocean-Ice Interactions Driving Arctic Sea Ice Response to CO_2 Increases. *J. Adv. Model. Earth Syst.*, **12**, doi:10.1029/2019MS001902.

Geen, R., S. I. Thomson, J. A. Screen, R. Blackport, N. T. Lewis, R. Mudhar, W. J. M. Seviour and G. K. Vallis, 2023: An explanation for the metric dependence of the midlatitude jet-waviness change in response to polar warming. *Geophys. Res. Lett.*, **50**, doi:10.1029/2023gl105132.

Gierens, R., S. Kneifel, M.D. Shupe, K. Ebell, M. Maturilli and U. Löhnert, 2020: Low-level mixed-phase clouds in a complex Arctic environment. *Atmos. Chem. Phys.*, **20**, 3459-3481.

Gong, X. D. and Coauthors, 2023: Arctic warming by abundant fine sea salt aerosols from blowing snow. *Nat. Geosci.*, **16**, 768-774.

Goosse, H., J. E. Kay, K. C. Armour, A. Bodas-Salcedo, H. Chepfer, D. Docquier, A. Jonko, P. J. Kushner, O. Lecomte, F. Massonnet, H. S. Park, F. Pithan, G. Svensson, and M. Vancoppenolle, 2018: Quantifying climate feedbacks in polar regions. *Nat. Commun.*, **9**, 1919, doi: doi.org/10.1038/s41467-018-04173-0.

Govin, A., P. Braconnot, E. Capron, E. Cortijo, J. C. Duplessy, E. Jansen, L. Labeyrie, A. Landais, O. Marti, E. Michel, E. Mosquet, B. Risebrobakken, D. Swingedouw, and C. Waelbroeck, 2012: Persistent influence of ice sheet melting on high northern latitude climate during the early Last Interglacial. *Clim. Past*, **8,** 483-507.

Graversen, R. G., and M. H. Wang, 2009: Polar amplification in a coupled climate model with locked albedo. *Clim. Dyn.*, **33,** 629-643.

Graversen, R. G., and M. Burtu, 2016: Arctic amplification enhanced by latent energy transport of atmospheric planetary waves. *Q. J. R. Meteorol. Soc.*, **142,** 2046–2054.

Griesche, H. J., C. Barrientos-Velasco, H. Deneke, A. Huenerbein, P. Seifert and A. Macke, 2024: Low-level Arctic clouds: a blind zone in our knowledge of the radiation budget. *Atmos. Chem. Phys.*, **24**, 597-612.

Guarino, M. V., L. C. Sime, R. Diamond, J. Ridley, and D. Schroeder, 2023: The coupled system response to 250 years of freshwater forcing: Last Interglacial CMIP6–PMIP4 HadGEM3 simulations. *Clim. Past*, **19,** 865-881.

Gulev, S. K., P. W. Thorne, J. Ahn, F. J. Dentener, C. M. Domingues, S. Gerland, D. Gong, D. S. Kaufman, H. C. Nnamchi, J. Quaas, J. A. Rivera, S. Sathyendranath, S. L. Smith, B. Trewin, K. v. Schuckmann, and R. S. Vose, 2021: Changing State of the Climate System. *Climate Change 2021: The Physical Science Basis.*, V. Masson-Delmotte, P. Zhai, A. Pirani, S.L. Connors, C. Péan, S. Berger, N. Caud, Y. Chen, L. Goldfarb, M.I. Gomis, M. Huang, K. Leitzell, E. Lonnoy,, and T. K. M. J.B.R. Matthews, T. Waterfield, O. Yelekçi, R. Yu, and B. Zhou, Eds., Cambridge University Press, 287–422.

Hahn, L. C., K. C. Armour, M. D. Zelinka, C. M. Bitz, and A. Donohoe, 2021: Contributions to Polar Amplification in CMIP5 and CMIP6 Models. *Frontiers in Earth Science*, **9**.

Haine, T. W. N., A. H. Siddiqui and W. R. Jiang, 2023: Arctic freshwater impact on the Atlantic Meridional Overturning Circulation: status and prospects. *Phil. Trans. Roy. Soc. A - Math. Phys. Eng. Sci.*, **381**, doi:10.1098/rsta.2022.0185.

Hall, A., 2004: The role of surface albedo feedback in climate. *J. Climate*, **17,** 1550-1568.

Hall, A., and S. Manabe, 1999: The role of water vapor feedback in unperturbed climate variability and global warming. *J. Climate*, **12,** 2327-2346.

Hanna, E. and Coauthors, 2024: Influence of high-latitude blocking and the northern stratospheric polar vortex on cold-air outbreaks under Arctic amplification of global warming. *Env. Res.-Climate*, **3**, doi:10.1088/2752-5295/ad93f3.

Hansen, J., M. Sato, G. Russell, and P. Kharecha, 2013: Climate sensitivity, sea level and atmospheric carbon dioxide. *Phil. Trans. R. Soc. A.*, **371**, 20120294, doi:10.1098/rsta.2012.0294.

Hay, S. and Coauthors, 2022: Separating the Influences of Low-Latitude Warming and Sea Ice Loss on Northern Hemisphere Climate Change. *J. Climate*, **35**, 2327-2349.

Haywood, A. M., H. J. Dowsett, J. C. Tindall, and P. a. P. participants, 2021: PlioMIP: The Pliocene Model Intercomparison Project. *PAGES Magazine*, **29**, 2, 92-93.

Haywood, A. M., H. J. Dowsett, M. M. Robinson, D. K. Stoll, A. M. Dolan, D. J. Lunt, B. Otto-Bliesner, and M. A. Chandler, 2011: Pliocene Model Intercomparison Project (PlioMIP): experimental design and boundary conditions (Experiment 2). *Geosci. Model Dev.*, **4,** 571-577.

Haywood, A. M., H. J. Dowsett, B. Otto-Bliesner, M. A. Chandler, A. M. Dolan, D. J. Hill, D. J. Lunt, M. M. Robinson, N. Rosenbloom, U. Salzmann, and L. E. Sohl, 2010: Pliocene Model Intercomparison Project (PlioMIP): experimental design and boundary conditions (Experiment 1). *Geosci. Model Dev.*, **3,** 227-242.

Haywood, A. M., H. J. Dowsett, A. M. Dolan, D. Rowley, A. Abe-Ouchi, B. Otto-Bliesner, M. A. Chandler, S. J. Hunter, D. J. Lunt, M. Pound, and U. Salzmann, 2016: The Pliocene Model Intercomparison Project (PlioMIP) Phase 2: scientific objectives and experimental design. *Clim. Past*, **12,** 663-675.

Haywood, A. M., J. C. Tindall, H. J. Dowsett, A. M. Dolan, K. M. Foley, S. J. Hunter, D. J. Hill, W.-L. Chan, A. Abe-Ouchi, C. Stepanek, G. Lohmann, D. Chandan, W. R. Peltier, N. Tan, C. Contoux, G. Ramstein, X. Li, Z. Zhang, C. Guo, K. H. Nisancioglu, Q. Zhang, Q. Li, Y. Kamae, M. A. Chandler, L. E. Sohl, B. L. Otto-Bliesner, R. Feng, E. C. Brady, A. S. von der Heydt, M. L. J. Baatsen, and D. J. Lunt, 2020: The Pliocene Model Intercomparison Project Phase 2: large-scale climate features and climate sensitivity. *Clim. Past*, **16,** 2095-2123.

Henderson, G. R., B. S. Barrett, L. J. Wachowicz, K. S. Mattingly, J. R. Preece, and T. L. Mote, 2021: Local and Remote Atmospheric Circulation Drivers of Arctic Change: A Review. *Front. in Earth Sci.*, **9**, doi:10.3389/feart.2021.709896.

Henry, M., and T. M. Merlis, 2019: The Role of the Nonlinearity of the Stefan-Boltzmann Law on the Structure of Radiatively Forced Temperature Change. *J. Climate*, **32,** 335-348.

Hersbach, H., B. Bell, P. Berrisford, S. Hirahara, A. Horányi, J. Muñoz-Sabater, J. Nicolas, C. Peubey, R. Radu, D. Schepers, A. Simmons, C. Soci, S. Abdalla, X. Abellan, G. Balsamo, P. Bechtold, G. Biavati, J. Bidlot, M. Bonavita, G. De Chiara, P. Dahlgren, D. Dee, M. Diamantakis, R. Dragani, J. Flemming, R. Forbes, M. Fuentes, A. Geer, L. Haimberger, S. Healy, R. J. Hogan, E. Hólm, M. Janisková, S. Keeley, P. Laloyaux, P. Lopez, C. Lupu, G. Radnoti, P. de Rosnay, I. Rozum, F. Vamborg, S. Villaume, and J. N.

Thépaut, 2020: The ERA5 global reanalysis. *Q. J. R. Meteorol. Soc.*, **146,** 1999-2049.

Heuzé, C., and M. Årthun, 2019: The Atlantic inflow across the Greenland-Scotland ridge in global climate models (CMIP5). *Elementa-Science of the Anthropocene*, **7**, 16, doi:10.1525/elementa.354.

Hill, D. J., A. M. Haywood, D. J. Lunt, S. J. Hunter, F. J. Bragg, C. Contoux, C. Stepanek, L. Sohl, N. A. Rosenbloom, W. L. Chan, Y. Kamae, Z. Zhang, A. Abe-Ouchi, M. A. Chandler, A. Jost, G. Lohmann, B. L. Otto-Bliesner, G. Ramstein, and H. Ueda, 2014: Evaluating the dominant components of warming in Pliocene climate simulations. *Clim. Past*, **10,** 79-90.

Hind, A., Q. Zhang, and G. Brattström, 2016: Problems encountered when defining Arctic amplification as a ratio. *Scientific Reports*, **6**, 30469, doi:10.1038/srep30469.

Hirose, L. A., A. Abe-Ouchi, W.-L. Chan, R. O'ishi, M. Yoshimori, and T. Obase 2025: Arctic warming suppressed by remnant glacial ice sheets in past interglacials. *Geophys. Res. Lett.*, in press.

Hoffman, J. S., P. U. Clark, A. C. Parnell, and F. He, 2017: Regional and global sea-surface temperatures during the last interglaciation. *Science*, **355,** 276-279.

Holland, M. M., and C. M. Bitz, 2003: Polar amplification of climate change in coupled models. *Clim. Dyn.*, **21,** 221-232.

Hopcroft, P. O., G. Ramstein, T. A. M. Pugh, S. J. Hunter, F. Murguia-Flores, A. Quiquet, Y. Sun, N. Tan, and P. J. Valdes, 2020: Polar amplification of Pliocene climate by elevated trace gas radiative forcing. *Proc. Natl. Acad. Sci. USA*, **117,** 23401-23407.

Hori, M. E., and M. Yoshimori, 2023: Assessment of the changing role of lower tropospheric temperature advection under arctic amplification using a large ensemble climate simulation dataset. *Clim. Dyn.*, **61,** 2355-2370.

Hori, M. E., M. Yoshimori, and J. Ukita, 2024: Changing role of horizontal moisture advection in the lower troposphere under extreme Arctic amplification. *Geophys. Res. Lett.*, **51,** e2024GL109299, doi:10.1029/2024GL109299.

Hu, X., Y. Liu, Y. Kong, and Q. Yang, 2022: A Quantitative Analysis of the Source of Inter-Model Spread in Arctic Surface Warming Response to Increased CO_2 Concentration. *Geophys. Res. Lett.*, **49**, e2022GL100034, doi:10.1029/2022GL100034.

Hu, X. M., P. C. Taylor, M. Cai, S. Yang, Y. Deng, and S. Sejas, 2017: Inter-Model Warming Projection Spread: Inherited Traits from Control Climate Diversity. *Scientific Reports*, **7**, 4300, doi:10.1038/s41598-017-04623-7.

Huber, M., and R. Caballero, 2011: The early Eocene equable climate problem revisited. *Clim. Past*, **7,** 603-633.

Hwang, Y. T., and D. M. W. Frierson, 2010: Increasing atmospheric poleward energy transport with global warming. *Geophys. Res. Lett.*, **37**, L24807, doi:10.1029/2010GL045440.

Hwang, Y. T., D. M. W. Frierson, and J. E. Kay, 2011: Coupling between Arctic feedbacks and changes in poleward energy transport. *Geophys. Res. Lett.*, **38,** L17704, doi:10.1029/2011GL048546.

ICS, 2023: International chronostratigraphic chart v 2023/09. International Commission on Stratigraphy (https://stratigraphy.org/chart).

Ingvaldsen, R. B., K. M. Assmann, R. Primicerio, M. Fossheim, I. V. Polyakov, and A. V. Dolgov, 2021: Physical manifestations and ecological implications of Arctic Atlantification. *Nat. Rev. Earth Environ.*, **2,** 874-889.

Intrieri, J.M., M. D. Shupe, T. Uttal, and B. J. McCarty, 2002: An annual cycle of Arctic cloud characteristics observed by radar and lidar at SHEBA. *J. Geophys. Res.*, **107**, doi:1029/2000JC000423.

Ishii, M., and M. Kimoto, 2009: Reevaluation of historical ocean heat content variations with time-varying XBT and MBT depth bias corrections. *J. Oceanography*, **65,** 287-299.

Ishii, M., Y. Fukuda, S. Hirahara, S. Yasui, T. Suzuki, and K. Sato, 2017: Accuracy of Global Upper Ocean Heat Content Estimation Expected from Present Observational Data Sets. *SOLA*, **13,** 163-167.

Jenkins, M., and A. G. Dai, 2021: The Impact of Sea-Ice Loss on Arctic Climate Feedbacks and Their Role for Arctic Amplification. *Geophys. Res. Lett.*, **48**, e2021GL094599, doi: 10.1029/2021GL094599.

Jenkins, M. T., and A. G. Dai, 2022: Arctic Climate Feedbacks in ERA5 Reanalysis: Seasonal and Spatial Variations and the Impact of Sea-Ice Loss. *Geophys. Res. Lett.*, **49**, e2022GL099263, doi:10.1029/2022GL099263.

Jiang, Z., C. Brierley, D. Thornalley, and S. Sax, 2023: No changes in overall AMOC strength in interglacial PMIP4 time slices. *Clim. Past*, **19,** 107-121.

Joussaume, S., and K. Taylor, 1995: *Status of the Paleoclimate Modeling Intercomparison Project. Proceedings of the First International AMIP Scientific Conference*, Monterey, USA, WCRP-92, 425-430.

Kacimi, S. and R. Kwok, 2022: Arctic snow depth, ice thickness, and volume from ICESat-2 and Crynat-2: 2018-2021. *Geophys. Res. Lett.*, **49**, doi:10.1029/2021gl097448.

Kageyama, M., L. C. Sime, M. Sicard, M.-V. Guarino, A. de Vernal, R. Stein, D. Schroeder, I. Malmierca-Vallet, A. Abe-Ouchi, C. Bitz, P. Braconnot, E. C. Brady, J. Cao, M. A. Chamberlain, D. Feltham, C. Guo, A. N. LeGrande, G. Lohmann, K. J. Meissner, L. Menviel, P. Morozova, K. H. Nisancioglu, B. L. Otto-Bliesner, R. O'Ishi, S. Ramos Buarque, D. Salas y Melia, S. Sherriff-Tadano, J. Stroeve, X. Shi, B. Sun, R. A. Tomas, E. Volodin, N. K. H. Yeung, Q. Zhang, Z. Zhang, W. Zheng, and T. Ziehn, 2021: A multi-model CMIP6-PMIP4 study of Arctic sea ice at 127 ka: sea ice data compilation and model differences. *Clim. Past*, **17,** 37-62.

Kaufman, D., N. McKay, C. Routson, M. Erb, C. Datwyler, P. S. Sommer, O. Heiri, and B. Davis, 2020: Holocene global mean surface temperature, a multi-method reconstruction approach. *Sci. Data*, **7,** 201, doi:10.1038/s41597-020-0530-.

Kaufman, D., 2023: Chapter 2 of the Working Group I Contribution to the IPCC Sixth Assessment Report - data for CCB 2.1, Figure 1 v20221114. NERC EDS Centre for

Environmental Data Analysis, 26 September 2023. doi:10.5285/0f05c2fb8f814d60ac2d657a70e9a7f5.

Kaufman, D. S., and E. Broadman, 2023: Revisiting the Holocene global temperature conundrum. *Nature*, **614,** 425-435.

Kawasaki, T., and H. Hasumi, 2016: The inflow of Atlantic water at the Fram Strait and its interannual variability. *J. Geophys. Res.-Oceans*, **121,** 502-519.

Kay, J. E., M. M. Holland and A. Jahn, 2011: Inter-annual to multi-decadal Arctic sea ice extent trends in a warming world. *Geophys. Res. Lett.*, **38**, doi:10.1029/2011gl048008.

Kay, J. E., T. L'Ecuyer, H. Chepfer, N. Loeb, A. Morrison and G. Cesana, 2016: Recent Advances in Arctic Cloud and Climate Research. *Curr. Clim. Chan. Rep.*, **2**, 159-169.

Kern, S., T. Lavergne, D. Notz, L. T. Pedersen and R. Tonboe, 2020: Satellite passive microwave sea-ice concentration data set inter-comparison for Arctic summer conditions. *Cryosphere*, **14**, 2469-2493.

Kern, S., T. Lavergne, D. Notz, L.T. Pedersen, R.T. Tonboe, R. Saldo and M. Sorensen, 2019: Satellite passive microwave sea-ice concentration data set intercomparison: closed ice and ship-based observations. *Cryosphere*, **13**, 3261-3307.

Klein, S. A., and Coauthors, 2009: Intercomparison of model simulations of mixed-phase clouds observed during the ARM Mixed-Phase Arctic Cloud Experiment. I: single-layer cloud. *Q. J. R. Meteorol. Soc.*, **135**, 979-1002.

Knies, J., P. Cabedo-Sanz, S. T. Belt, S. Baranwal, S. Fietz, and A. Rosell-Melé, 2014: The emergence of modern sea ice cover in the Arctic Ocean. *Nat. Commun.*, **5**, 5608, doi: 10.1038/ncomms6608.

Kodaira, T., T. Waseda, T. Nose and J. Inoue, 2020: Record high Pacific Arctic seawater temperatures and delayed sea ice advance in response to episodic atmospheric blocking. *Sci. Rep.*, **10**, doi:10.1038/s41598-020-77488-y.

Koenigk, T., and L. Brodeau, 2017: Arctic climate and its interaction with lower latitudes under different levels of anthropogenic warming in a global coupled climate model. *Clim. Dyn.*, **49,** 471-492.

Kohyama, T., Y. Yamagami, H. Miura, S. Kido, H. Tatebe and M. Watanabe, 2021: The Gulf Stream and Kuroshio Current are synchronized. *Science*, **374**, 341-346.

Kwok, R., 2018: Arctic sea ice thickness, volume, and multiyear ice coverage: losses and coupled variability (1958-2018). *Env. Res. Lett.*, **13**, doi:10.1088/1748-9326/aae3ec.

Kwok, R., S. Kacimi, M.A. Webster, N.T. Kurtz and A.A. Petty, 2020: Arctic snow depth and sea ice thickness from ICESat-2 and CryoSat-2 freeboards: A first examination. *J. Geophys. Res.*, **125**, doi:10.1029/2019jc016008.

Laîné, A., M. Yoshimori, and A. Abe-Ouchi, 2016: Surface Arctic amplification factors in CMIP5 models: land and oceanic surfaces, seasonality. *J. Climate*, **29**, 3297–3316.

Langen, P. L., R. G. Graversen, and T. Mauritsen, 2012: Separation of contributions from radiative feedbacks to polar amplification on an aquaplanet. *J. Climate*, **25,** 3010-3024.

Lee, Y. C., W. Liu, A. Fedorov, N. Feldl and P. C. Taylor, 2024: Impacts of Atlantic meridional overturning circulation weakening on Arctic amplification. *Proc. Natl. Acad. Sci. USA*, **121**, doi:10.1073/pnas.2402322121.

Li, Z., Q. H. Ding, M. Steele, and A. Schweiger, 2022: Recent upper Arctic Ocean warming expedited by summertime atmospheric processes. *Nat. Commun.*, **13**, 362, doi: 10.1038/s41467-022-28047-8.

Liang, Y., H. B. Bi, R. B. Lei, T. Vihma, and H. J. Huang, 2023: Atmospheric Latent Energy Transport Pathways into the Arctic and Their Connections to Sea Ice Loss during Winter over the Observational Period. *J. Climate*, **36,** 6695-6712.

Liu, Y., M. Zhang, Z. Liu, Y. Xia, Y. Huang, Y. Peng, and J. Zhu, 2018: A Possible Role of Dust in Resolving the Holocene Temperature Conundrum. *Sci Rep*, **8,** 4434, doi:10.1038/s41598-018-22841-5.

Liu, Z. and Coauthors, 2022: Atmospheric forcing dominates winter Barents-Kara sea ice variability on interannual to decadal time scales. *Proc. Natl. Acad. Sci. USA*, **119**, doi:10.1073/pnas.2120770119.

Liu, Z., J. Zhu, Y. Rosenthal, X. Zhang, B. L. Otto-Bliesner, A. Timmermann, R. S. Smith, G. Lohmann, W. Zheng, and O. E. Timm, 2014: The Holocene temperature conundrum. *Proc. Natl. Acad. Sci. USA*, **111,** E3501-3505, doi:10.1073/pnas.1407229111.

Lu, J. H., and M. Cai, 2009a: A new framework for isolating individual feedback processes in coupled general circulation climate models. Part I: formulation. *Clim. Dyn.*, **32,** 873-885.

Lu, J. H., and M. Cai, 2009b: Seasonality of polar surface warming amplification in climate simulations. *Geophys. Res. Lett.*, **36**, L16704, doi:10.1029/2009GL040133.

Lu, J. H., and M. Cai, 2010: Quantifying contributions to polar warming amplification in an idealized coupled general circulation model. *Clim. Dyn.*, **34,** 669-687.

Lunt, D. J., A. M. Haywood, G. L. Foster, and E. J. Stone, 2009: The Arctic cryosphere in the Mid-Pliocene and the future. *Philos. Transact. A Math. Phys. Eng. Sci.*, **367,** 49-67.

Lunt, D. J., A. M. Haywood, G. A. Schmidt, U. Salzmann, P. J. Valdes, H. J. Dowsett, and C. A. Loptson, 2012: On the causes of mid-Pliocene warmth and polar amplification. *Earth Planet. Sci. Lett.*, **321-322,** 128-138.

Lunt, D. J., A. Abe-Ouchi, P. Bakker, A. Berger, P. Braconnot, S. Charbit, N. Fischer, N. Herold, J. H. Jungclaus, V. C. Khon, U. Krebs-Kanzow, P. M. Langebroek, G. Lohmann, K. H. Nisancioglu, B. L. Otto-Bliesner, W. Park, M. Pfeiffer, S. J. Phipps, M. Prange, R. Rachmayani, H. Renssen, N. Rosenbloom, B. Schneider, E. J. Stone, K. Takahashi, W. Wei, Q. Yin, and Z. S. Zhang, 2013: A multi-model assessment of last interglacial temperatures. *Clim. Past*, **9,** 699-717.

Lunt, D. J., F. Bragg, W. L. Chan, D. K. Hutchinson, J. B. Ladant, P. Morozova, I. Niezgodzki, S. Steinig, Z. S. Zhang, J. Zhu, A. Abe-Ouchi, E. Anagnostou, A. M. de Boer, H. K. Coxall, Y. Donnadieu, G. Foster, G. N. Inglis, G. Knorr, P. M. Langebroek, C. H. Lear, G. Lohmann, C. J. Poulsen, P. Sepulchre, J. E. Tierney, P. J. Valdes, E. M. Volodin, T. D. Jones, C. J. Hollis, M. Huber, and B. L. Otto-Bliesner, 2021: DeepMIP: model intercomparison of early Eocene climatic optimum (EECO) large-scale climate features and comparison with proxy data. *Clim. Past*, **17,** 203-227.

Mahlstein, I., and R. Knutti, 2011: Ocean Heat Transport as a Cause for Model Uncertainty in Projected Arctic Warming. *J. Climate*, **24,** 1451-1460.

Manabe, S., and R. T. Wetherald, 1975: Effects of doubling CO_2 concentration on climate of a general circulation model. *J. Atmos. Sci.*, **32,** 3-15.

Manabe, S., and R. J. Stouffer, 1979: CO_2-climate sensitivity study with a mathematical-model of the global climate. *Nature*, **282,** 491-493.

Marcott, S. A., J. D. Shakun, P. U. Clark, and A. C. Mix, 2013: A reconstruction of regional and global temperature for the past 11,300 years. *Science*, **339,** 1198-1201.

Marsicek, J., B. N. Shuman, P. J. Bartlein, S. L. Shafer, and S. Brewer, 2018: Reconciling divergent trends and millennial variations in Holocene temperatures. *Nature*, **554,** 92-96.

Matsui, H., K. Kawai, Y. Tobo, Y. Iizuka and S. Matoba, 2024: Increasing Arctic dust suppresses the reduction of ice nucleation in the Arctic lower troposphere by warming. *Npj Clim. Atmos. Sci.*, **7**, doi:10.1038/s41612-024-00811-1.

Mayer, M., S. Tietsche, L. Haimberger, T. Tsubouchi, J. Mayer, and H. Zuo, 2019: An Improved Estimate of the Coupled Arctic Energy Budget. *J. Climate*, **32,** 7915-7934.

McClymont, E. L., H. L. Ford, S. L. Ho, J. C. Tindall, A. M. Haywood, M. Alonso-Garcia, I. Bailey, M. A. Berke, K. Littler, M. O. Patterson, B. Petrick, F. Peterse, A. C. Ravelo, B. Risebrobakken, S. De Schepper, G. E. A. Swann, K. Thirumalai, J. E. Tierney, C. van der Weijst, S. White, A. Abe-Ouchi, M. L. J. Baatsen, E. C. Brady, W.-L. Chan, D. Chandan, R. Feng, C. Guo, A. S. von der Heydt, S. Hunter, X. Li, G. Lohmann, K. H. Nisancioglu, B. L. Otto-Bliesner, W. R. Peltier, C. Stepanek, and Z. Zhang, 2020: Lessons from a high-CO_2 world: An ocean view from ~3 million years ago. *Clim. Past*, **16,** 1599-1615.

McKay, N. P., J. T. Overpeck, and B. L. Otto-Bliesner, 2011: The role of ocean thermal expansion in Last Interglacial sea level rise. *Geophys. Res. Lett.*, **38,** L14605, doi:10.1029/2011GL048280.

Michel, S. L. L., A. S. von der Heydt, R. M. van Westen, M. L. J. Baatsen, and H. A. Dijkstra, 2023: Increased wintertime European atmospheric blocking frequencies in General Circulation Models with an eddy-permitting ocean. *Npj Clim. Atmos. Sci.*, **6**, 50, doi:10.1038/s41612-023-00372-9.

Michibata, T., 2024: Radiative effects of precipitation on the global energy budget and Arctic amplification. *Npj Clim. Atmos. Sci.*, **7**, doi:10.1038/s41612-024-00684-4.

Middlemas, E. A., J. E. Kay, B. M. Medeiros, and E. A. Maroon, 2020: Quantifying the Influence of Cloud Radiative Feedbacks on Arctic Surface Warming Using Cloud Locking in an Earth System Model. *Geophys. Res. Lett.*, **47**, e2020GL089207, doi:10.1029/2020GL089207.

Miles, M. W., D. V. Divine, T. Furevik, E. Jansen, M. Moros and A. E.J. Ogilvie, 2014: A signal of persistent Atlantic multidecadal variability in Arctic sea ice. *Geophys. Res. Lett.*,

41, 463-469.

Mori, M., M. Watanabe, H. Shiogama, J. Inoue and M. Kimoto, 2014: Robust Arctic sea-ice influence on the frequent Eurasian cold winters in past decades. *Nat. Geosci.*, **7**, 869-873.

Mori, M., Y. Kosaka, M. Watanabe, H. Nakamura and M. Kimoto, 2019: A reconciled estimate of the influence of Arctic sea-ice loss on recent Eurasian cooling. *Nat. Clim. Chan.*, **9**, 123-129.

Morice, C.P. and Coauthors, 2021: An Updated Assessment of Near-Surface Temperature Change From 1850: The HadCRUT5 Data Set. J. of Geophys. Res., 126, ARTN e2019JD032361, doi:10.1029/2019JD032361.

Morrison, H., G. de Boer, G. Feingold, J. Harrington, M. D. Shupe and K. Sulia, 2011a: Resilience of persistent Arctic mixed-phase clouds. *Nat. Geosci.*, **5**, 11-17.

Morrison, H., and Coauthors, 2011b: Intercomparison of cloud model simulations of Arctic mixed-phase boundary layer clouds observed during SHEBA/FIRE-ACE. *J. Adv. Model. Earth Syst.*, **3**, Art. 306003, doi:10.1029/2011MS000066.

Morrison, H., and Coauthors, 2009: Intercomparison of model simulations of mixed-phase clouds observed during the ARM Mixed-Phase Arctic Cloud Experiment. II: Multilayer cloud. Q. J. R. Meteorol. Soc., **135**, 1003-1019.

Murray, B. J., K. S. Carslaw, and P. R. Field, 2021: Opinion: Cloud-phase climate feedback and the importance of ice-nucleating particles. *Atmos. Chem. Phys.*, **21,** 665-679.

Nakamura, T., K. Yamazaki, K. Iwamoto, M. Honda, Y. Miyoshi, Y. Ogawa, and J. Ukita, 2015: A negative phase shift of the winter AO/NAO due to the recent Arctic sea-ice reduction in late autumn. *J. Geophys. Res.-Atmospheres*, **120,** 3209-3227.

Nakamura, T., K. Yamazaki, K. Iwamoto, M. Honda, Y. Miyoshi, Y. Ogawa, Y. Tomikawa and J. Ukita, 2016: The stratospheric pathway for Arctic impacts on midlatitude climate. *Geophys. Res. Lett.*, **43**, 3494-3501.

Nakanowatari, T., J. Inoue, J.L. Zhang, E. Watanabe and H. Kuroda, 2022: A new norm for seasonal sea ice advance predictability in the Chukchi Sea: Rising influence of ocean heat advection. *J. Climate*, **35**, 2723-2740.

Nicolaus, M., and Coauthors, 2022: Overview of the MOSAiC expedition: Snow and sea ice. *Elem. Sci. Anth.*, **10**, doi:10.1525/elementa.2021.000046.

Niezgodzki, I., G. Knorr, G. Lohmann, D. J. Lunt, C. J. Poulsen, S. Steinig, J. Zhu, A. de Boer, W. L. Chan, Y. Donnadieu, D. K. Hutchinson, J. B. Ladant, and P. Morozova, 2022: Simulation of Arctic sea ice within the DeepMIP Eocene ensemble: Thresholds, seasonality and factors controlling sea ice development. *Glob. Planet. Change*, **214**, doi:10.1016/j.gloplacha.2022.103848.

Nummelin, A., C. Li, and P. J. Hezel, 2017: Connecting ocean heat transport changes from the midlatitudes to the Arctic Ocean. *Geophys. Res. Lett.*, **44,** 1899-1908.

O'ishi, R., and A. Abe-Ouchi, 2009: Influence of dynamic vegetation on climate change arising from increasing CO2. *Clim. Dyn.*, **33,** 645-663.

O'ishi, R., and A. Abe-Ouchi, 2011: Polar amplification in the mid-Holocene derived from dynamical vegetation change with a GCM. *Geophys. Res. Lett.*, **38,** L14702, doi:10.1029/2011GL048001.

O'ishi, R., A. Abe-Ouchi, I. C. Prentice, and S. Sitch, 2009: Vegetation dynamics and plant CO_2responses as positive feedbacks in a greenhouse world. *Geophys. Res. Lett.*, **36**, L11706, doi:10.1029/2009GL038217.

O'ishi, R., W.-L. Chan, A. Abe-Ouchi, S. Sherriff-Tadano, R. Ohgaito, and M. Yoshimori, 2021: PMIP4/CMIP6 last interglacial simulations using three different versions of MIROC: importance of vegetation. *Clim. Past*, **17,** 21-36.

Obase, T., and A. Abe-Ouchi, 2019: Abrupt Bølling-Allerød Warming Simulated under Gradual Forcing of the Last Deglaciation. *Geophys. Res. Lett.*, **46,** 11397-11405.

Obase, T., A. Abe-Ouchi, and F. Saito, 2021: Abrupt climate changes in the last two deglaciations simulated with different Northern ice sheet discharge and insolation. *Sci. Rep.*, **11,** 22359, doi:10.1038/s41598-021-01651-2.

Ohmura, A., 1984: On the Cause of Fram Type Seasonal Change in Diurnal Amplitude of Air-Temperature in Polar-Regions. *J. Climatol.*, **4,** 325-338.

Ohmura, A., 2012: Enhanced temperature variability in high-altitude climate change. *Theor. Appl. Climatol.*, **110,** 499-508.

Onuma, Y., K. Yoshimura and N. Takeuchi, 2022: Global Simulation of Snow Algal Blooming by Coupling a Land Surface and Newly Developed Snow Algae Models. *J.*

Geophys. Res., **127**, doi:0.1029/2021jg006339.

Osman, M. B., J. E. Tierney, J. Zhu, R. Tardif, G. J. Hakim, J. King, and C. J. Poulsen, 2021: Globally resolved surface temperatures since the Last Glacial Maximum. *Nature*, **599,** 239-244.

Otto, J., T. Raddatz, M. Claussen, V. Brovkin, and V. Gayler, 2009: Separation of atmosphere-ocean-vegetation feedbacks and synergies for mid-Holocene climate. *Geophys. Res. Lett.*, **36**, L09701, doi:10.1029/2009GL037482.

Otto-Bliesner, B. L., S. J. Marshall, J. T. Overpeck, G. H. Miller, and A. Hu, 2006: Simulating Arctic climate warmth and icefield retreat in the last interglaciation. *Science*, **311,** 1751-1753.

Otto-Bliesner, B. L., N. Rosenbloom, E. J. Stone, N. P. McKay, D. J. Lunt, E. C. Brady, and J. T. Overpeck, 2013: How warm was the last interglacial? New model-data comparisons. *Philos. Trans. A Math. Phys. Eng. Sci.*, **371,** 20130097, doi:10.1098/rsta.2013.0097.

Otto-Bliesner, B. L., P. Braconnot, S. P. Harrison, D. J. Lunt, A. Abe-Ouchi, S. Albani, P. J. Bartlein, E. Capron, A. E. Carlson, A. Dutton, H. Fischer, H. Goelzer, A. Govin, A. Haywood, F. Joos, A. N. LeGrande, W. H. Lipscomb, G. Lohmann, N. Mahowald, C. Nehrbass-Ahles, F. S. R. Pausata, J.-Y. Peterschmitt, S. J. Phipps, H. Renssen, and Q. Zhang, 2017: The PMIP4 contribution to CMIP6 – Part 2: Two interglacials, scientific objective and experimental design for Holocene and Last Interglacial simulations.

Geosci. Model Dev., **10,** 3979-4003.

Otto-Bliesner, B. L., E. C. Brady, A. Zhao, C. M. Brierley, Y. Axford, E. Capron, A. Govin, J. S. Hoffman, E. Isaacs, M. Kageyama, P. Scussolini, P. C. Tzedakis, C. J. R. Williams, E. Wolff, A. Abe-Ouchi, P. Braconnot, S. Ramos Buarque, J. Cao, A. de Vernal, M. V. Guarino, C. Guo, A. N. LeGrande, G. Lohmann, K. J. Meissner, L. Menviel, P. A. Morozova, K. H. Nisancioglu, R. O'Ishi, D. Salas y Mélia, X. Shi, M. Sicard, L. Sime, C. Stepanek, R. Tomas, E. Volodin, N. K. H. Yeung, Q. Zhang, Z. Zhang, and W. Zheng, 2021: Large-scale features of Last Interglacial climate: results from evaluating the lig127k simulations for the Coupled Model Intercomparison Project (CMIP6)–Paleoclimate Modeling Intercomparison Project (PMIP4). *Clim. Past*, **17,** 63-94.

Outten, S. and Coauthors, 2023: Reconciling conflicting evidence for the cause of the observed early 21st century Eurasian cooling. *Weather and Clim. Dyn.*, **4**, 95-114.

Ovchinnikov, M., and Coauthors, 2014: Intercomparison of large-eddy simulations of Arctic mixed-phase clouds: Importance of ice size distribution assumptions. *J. Adv. Model. Earth Syst.,* **6**, 223-248.

Park, H.-S., S. Lee, Y. Kosaka, S.-W. Son, and S.-W. Kim, 2015a: The Impact of Arctic Winter Infrared Radiation on Early Summer Sea Ice. *J. Climate*, **28,** 6281-6296.

Park, H.-S., S. Lee, S.-W. Son, S. B. Feldstein, and Y. Kosaka, 2015b: The Impact of Poleward Moisture and Sensible Heat Flux on Arctic Winter Sea Ice Variability. *J. Climate*, **28,** 5030-5040.

Park, H., Y. Kim, K. Suzuki and T. Hiyama, 2024: Influence of snowmelt on increasing Arctic river discharge: numerical evaluation. *Prog. Earth Planet. Sci.*, **11**, doi:10.1186/s40645-024-00617-y.

Pedersen, R. A., P. L. Langen, and B. M. Vinther, 2016: The last interglacial climate: comparing direct and indirect impacts of insolation changes. *Clim. Dyn.*, **48,** 3391-3407.

Peralta-Ferriz, C., and R. A. Woodgate, 2023: Arctic and Sub-Arctic Mechanisms Explaining Observed Increasing Northward Flow Through the Bering Strait and Why Models May Be Getting It Wrong. *Geophys. Res. Lett.*, **50**, e2023GL104697, doi:10.1029/2023GL104697.

Perovich, D. K., 2002: Seasonal evolution of the albedo of multiyear Arctic sea ice. *J. Geophys. Res.*, **107**, 8044, doi:10.1029/2000JC000438.

Perovich, D. K., and C. Polashenski, 2012: Albedo evolution of seasonal Arctic sea ice. *Geophys. Res. Lett.*, **39**, L08501, doi:10.1029/2012GL051432.

Pithan, F., and T. Mauritsen, 2014: Arctic amplification dominated by temperature feedbacks in contemporary climate models. *Nat. Geosci.*, **7,** 181-184.

Pithan, F., B. Medeiros, and T. Mauritsen, 2014: Mixed-phase clouds cause climate model biases in Arctic wintertime temperature inversions. *Clim. Dyn.*, **43**, 289-303.

Polyak, L., R. B. Alley, J. T. Andrews, J. Brigham-Grette, T. M. Cronin, D. A. Darby, A. S. Dyke, J. J. Fitzpatrick, S. Funder, M. Holland, A. E. Jennings, G. H. Miller, M. O'Regan, J. Savelle, M. Serreze, K. St. John, J. W. C. White, and E. Wolff, 2010: History of sea ice in the Arctic. *Quat. Sci. Rev.*, **29,** 1757-1778.

Polyakov, I. V., A. V. Pnyushkov, and E. C. Carmack, 2018: Stability of the arctic halocline: a new indicator of arctic climate change. *Environ. Res. Lett.*, **13**, 125008, doi:10.1088/1748-9326/aaec1e.

Polyakov, I. V., L. Padman, Y. D. Lenn, A. Pnyushkov, R. Rember, and V. V. Ivanov, 2019: Eastern Arctic Ocean Diapycnal Heat Fluxes through Large Double-Diffusive Steps. *J. Phys. Oceanogr.*, **49,** 227-246.

Polyakov, I. V., T. P. Rippeth, I. Fer, T. M. Baumann, E. C. Carmack, V. V. Ivanov, M. Janout, L. Padman, A. V. Pnyushkov, and R. Rember, 2020a: Intensification of Near-Surface Currents and Shear in the Eastern Arctic Ocean. *Geophys. Res. Lett.*, **47**, e2020GL089469, doi:10.1029/2020GL089469.

Polyakov, I. V., M. B. Alkire, B. A. Bluhm, K. A. Brown, E. C. Carmack, M. Chierici, S. L. Danielson, I. Ellingsen, E. A. Ershova, K. Gårdfeldt, R. B. Ingvaldsen, A. V. Pnyushkov, D. Slagstad, and P. Wassmann, 2020b: Borealization of the Arctic Ocean in Response to Anomalous Advection From Sub-Arctic Seas. *Front. Mar. Sci.*, **7**, doi:10.3389/fmars.2020.00491.

Polyakov, I. V., A. V. Pnyushkov, M. B. Alkire, I. M. Ashik, T. M. Baumann, E. C. Carmack, I. Goszczko, J. Guthrie, V. V. Ivanov, T. Kanzow, R. Krishfield, R. Kwok, A. Sundfjord, J. Morison, R. Rember, and A. Yulin, 2017: Greater role for Atlantic inflows on sea-ice loss in the Eurasian Basin of the Arctic Ocean. *Science*, **356,** 285-291.

Polyakov, I. V., T. P. Rippeth, I. Fer, M. B. Alkire, T. M. Baumann, E. C. Carmack, R. Ingvaldsen, V. V. Ivanov, M. Janout, S. Lind, L. Padman, A. V. Pnyushkov, and R. Rember, 2020c: Weakening of Cold Halocline Layer Exposes Sea Ice to Oceanic Heat in the Eastern Arctic Ocean. *J. Climate*, **33,** 8107-8123.

Pontes, G. M. and L. Menviel, 2024: Weakening of the Atlantic Meridional Overturning Circulation driven by subarctic freshening since the mid-twentieth century. *Nat. Geosci.*, **17**, doi:10.1038/s41561-024-01568-1.

Previdi, M., K. L. Smith, and L. M. Polvani, 2021: Arctic amplification of climate change: a review of underlying mechanisms. *Environ. Res. Lett.*, **16**, 093003, doi:10.1088/1748-9326/ac1c29.

Rabe, B., and Coauthors, 2022: Overview of the MOSAiC expedition: Physical oceanography. *Elem. Sci. Anth.*, **10**, doi:10.1525/elementa.2021.00062.

Rantanen, M., A. Y. Karpechko, A. Lipponen, K. Nordling, O. Hyvärinen, K. Ruosteenoja, T. Vihma, and A. Laaksonen, 2022: The Arctic has warmed nearly four times faster than the globe since 1979. *Commun. Earth Environ.*, **3**, 168, doi:10.1038/s43247-022-00498-3.

Raymo, M. E., B. Grant, M. Horowitz, and G. H. Rau, 1996: Mid-Pliocene warmth: stronger greenhouse and stronger conveyor. *Mar. Micropaleontol.*, **27,** 313-326.

Rudels, B., and E. Carmack, 2022: Arctic Ocean Water Mass Structure and Circulation. *Oceanography*, **35**, 52-65.

Rydsaa, J. H., R. G. Graversen, T. I. H. Heiskanen, and P. J. Stoll, 2021: Changes in atmospheric latent energy transport into the Arctic: Planetary versus synoptic scales. *Q. J. R. Meteorol. Soc.*, **147,** 2281-2292.

Saenko, O. A., J. M. Gregory, and N. F. Tandon, 2024: Uncertainties in the Arctic Ocean response to CO_2: a process-based analysis. *Clim. Dyn.*, **62,** 1649-1668.

Sagoo, N., T. Storelvmo, L. Hahn, I. Tan, J. Danco, B. Raney, and A. J. Broccoli, 2021: Observationally constrained cloud phase unmasks orbitally driven climate feedbacks. *Geophys. Res. Lett.*, **48**, e2020GL091873, doi:10.1029/2020GL091873.

Salzmann, U., A. M. Dolan, A. M. Haywood, W.-L. Chan, J. Voss, D. J. Hill, A. Abe-Ouchi, B. Otto-Bliesner, F. J. Bragg, M. A. Chandler, C. Contoux, H. J. Dowsett, A. Jost, Y. Kamae, G. Lohmann, D. J. Lunt, S. J. Pickering, M. J. Pound, G. Ramstein, N. A. Rosenbloom, L. Sohl, C. Stepanek, H. Ueda, and Z. Zhang, 2013: Challenges in quantifying Pliocene terrestrial warming revealed by data–model discord. *Nat. Clim. Change*, **3,** 969-974.

Sang, X. Z., X. Q. Yang, L. F. Tao, J. B. Fang and X. G. Sun, 2022: Decadal changes of wintertime poleward heat and moisture transport associated with the amplified Arctic warming. *Clim. Dyn.*, **58**, 137-159.

Sato, K., J. Inoue and M. Watanabe, 2014: Influence of the Gulf Stream on the Barents Sea ice retreat and Eurasian coldness during early winter. Env. Res. Lett., **9**, doi:10.1088/1748-9326/9/8/084009.

Schmidt, G. A., J. D. Annan, P. J. Bartlein, B. I. Cook, E. Guilyardi, J. C. Hargreaves, S. P. Harrison, M. Kageyama, A. N. LeGrande, B. Konecky, S. Lovejoy, M. E. Mann, V. Masson-Delmotte, C. Risi, D. Thompson, A. Timmermann, L. B. Tremblay, and P. Yiou, 2014: Using palaeo-climate comparisons to constrain future projections in CMIP5. *Clim. Past*, **10,** 221-250.

Schneider, E. K., B. P. Kirtman, and R. S. Lindzen, 1999: Tropospheric water vapor and climate sensitivity. *J. Atmos. Sci.*, **56,** 1649-1658.

Screen, J. A., and I. Simmonds, 2010: The central role of diminishing sea ice in recent Arctic temperature amplification. *Nature*, **464,** 1334-1337.

Sedlar, J., and Coauthors, 2020: Confronting Arctic troposphere, clouds, and surface energy budget representations in regional climate models with observations. *J. Geophys. Res.*, **124**, doi:10.1029/2019JD031783.

Screen, J. A. and J. A. Francis, 2016: Contribution of sea-ice loss to Arctic amplification is regulated by Pacific Ocean decadal variability. *Nat. Clim. Chan.*, 6, 856-860.

Screen, J. A., T. J. Bracegirdle and I. Simmonds, 2018a: Polar Climate Change as Manifest in Atmospheric Circulation. *Curr. Clim. Chan. Rep.*, **4**, 383-395.

Screen, J. A., C. Deser, D. M. Smith, X. D. Zhang, R. Blackport, P. J. Kushner, T. Oudar, K. E. McCusker and L. T. Sun, 2018b: Consistency and discrepancy in the atmospheric response to Arctic sea-ice loss across climate models. *Nat. Geosci.*, **11**, 155-163.

Sejas, S. A., X. M. Hu, M. Cai, and H. J. Fan, 2021: Understanding the differences between TOA and surface energy budget attributions of surface warming. *Front. Earth Sci.*, **9**, doi:10.3389/feart.2021.725816.

Semenov, V. A., 2021: Modern Arctic climate research: Progress, change of concepts, and urgent problems. *Izvestiya Atmospheric and Oceanic Physics*, **57,** 18-28.

Serreze, M. C., and J. A. Francis, 2006: The Arctic amplification debate. *Clim. Change*, **76,** 241-264.

Serreze, M. C., and R. G. Barry, 2011: Processes and impacts of Arctic amplification: A research synthesis. *Glob. Planet. Change*, **77,** 85-96.

Serreze, M. C., A. P. Barrett, J. C. Stroeve, D. N. Kindig, and M. M. Holland, 2009: The emergence of surface-based Arctic amplification. *Cryosphere*, **3,** 11-19.

Shakun, J. D., P. U. Clark, F. He, S. A. Marcott, A. C. Mix, Z. Liu, B. Otto-Bliesner, A. Schmittner, and E. Bard, 2012: Global warming preceded by increasing carbon dioxide concentrations during the last deglaciation. *Nature*, **484,** 49-54.

Shen, Z. L., A. M. Duan, W. Zhou, Y. Z. Peng and J. X. Li, 2024: Reconciling Roles of External Forcing and Internal Variability in Arctic Sea Ice Change on Different Time Scales. *J. Climate*, **37**, 3577-3591.

Sherriff-Tadano, S., A. Abe-Ouchi, M. Yoshimori, R. Ohgaito, T. Vadsaria, W. L. Chan, H. Hotta, M. Kikuchi, T. Kodama, A. Oka, and K. Suzukia, 2023: Southern Ocean surface temperatures and cloud biases in climate models connected to the representation of glacial deep ocean circulation. *J. Climate*, **36,** 3849-3866.

Sherwood, S. C., M. J. Webb, J. D. Annan, K. C. Armour, P. M. Forster, J. C. Hargreaves, G. Hegerl, S. A. Klein, K. D. Marvel, E. J. Rohling, M. Watanabe, T. Andrews, P. Braconnot, C. S. Bretherton, G. L. Foster, Z. Hausfather, A. S. Heydt, R. Knutti, T. Mauritsen, J. R. Norris, C. Proistosescu, M. Rugenstein, G. A. Schmidt, K. B. Tokarska, and M. D. Zelinka, 2020: An assessment of Earth's climate sensitivity using multiple lines of evidence. *Rev. Geophys.*, **58**, e2019RG000678, doi:10.1029/2019RG000678.

Shu, Q., Q. Wang, M. Arthun, S. Wang, Z. Song, M. Zhang, and F. Qiao, 2022: Arctic Ocean amplification in a warming climate in CMIP6 models. *Sci Adv*, **8,** doi:10.1126/sciadv.abn9.

Shupe, M. D., T. Uttal, S. Y. Matrosov, and A. S. Frisch, 2001: Cloud water contents and hydrometeor sizes during the FIRE Arctic Clouds Experiment. *J. Geophys. Res.*, **106**, 15015-15028.

Shupe, M. D., and Coauthors, 2022: Overview of the MOSAiC expedition: Atmosphere. *Elem. Sci. Anth.*, **10**, doi:10.1525/elementa.2021.00060.

Sicard, M., M. Kageyama, S. Charbit, P. Braconnot, and J.-B. Madeleine, 2022: An energy budget approach to understand the Arctic warming during the Last Interglacial. *Clim. Past*, **18,** 607-629.

Siew, P. Y. F., Y. T. Wu, M. F. Ting, C. Zheng, Q. H. Ding and R. Seager, 2024: Significant contribution of internal variability to recent Barents-Kara sea ice loss in winter. *Commun. Earth Environ.*, **5**, doi:10.1038/s43247-024-01582-6.

Sigmond, M. and L. Sun, 2024: The role of the basic state in the climate response to future Arctic sea ice loss. *Env. Res.-Climate*, **3**, doi:10.1088/2752-5295/ad44ca.

Sime, L. C., R. Sivankutty, I. Vallet-Malmierca, A. M. de Boer, and M. Sicard, 2023: Summer surface air temperature proxies point to near-sea-ice-free conditions in the Arctic at 127 ka. *Clim. Past*, **19,** 883-900.

Singh, H. A., P. J. Rasch, and B. E. J. Rose, 2017: Increased ocean heat convergence into the high latitudes with CO_2 doubling enhances polar-amplified warming. *Geophys. Res. Lett.*, **44,** 10,583-510,591.

Skiles, S. M., M. Flanner, J. M. Cook, M. Dumont and T. H. Painter, 2018: Radiative forcing by light-absorbing particles in snow. *Nat. Clim. Chan.*, 8, 965-971.

Smith, D. M. and Coauthors, 2022: Robust but weak winter atmospheric circulation response to future Arctic sea ice loss. *Nat. Comm.*, **13**, doi:10.1038/s41467-022-28283-y.

Snyder, C. W., 2016: Evolution of global temperature over the past two million years. *Nature*, **538,** 226-228.

Song, Z., M. Latif, W. Park, and Y. Zhang, 2018: Influence of model bias on simulating North Atlantic sea surface temperature during the mid-Pliocene. *Paleoceanogr. Paleoclimatol.*, **33,** 884-893.

Stevens, R. G., and Coauthors, 2018: A model intercomparison of CCN-limited tenuous clouds in the high Arctic. *Atmos. Chem. Phys.*, **18**, 11041-11071.

Stuecker, M. F., C. M. Bitz, K. C. Armour, C. Proistosescu, S. M. Kang, S. P. Xie, D. Kim, S. McGregor, W. J. Zhang, S. Zhao, W. J. Cai, Y. Dong, and F. F. Jin, 2018: Polar amplification dominated by local forcing and feedbacks. *Nat. Clim. Change*, **8,** 1076-1081.

Sundqvist, H. S., Q. Zhang, A. Moberg, K. Holmgren, H. Körnich, J. Nilsson, and G. Brattström, 2010: Climate change between the mid and late Holocene in northern high latitudes – Part 1: Survey of temperature and precipitation proxy data. *Clim. Past*, **6,** 591-608.

Svendsen, L., N. Keenlyside, I. Bethke, Y. Q. Gao and N. E. Omrani, 2018: Pacific contribution to the early twentieth-century warming in the Arctic. *Nat. Clim. Chan.*, **8**, 793-797.

Sweeney, A. J., Q. Fu, S. Po-Chedley, H. L. Wang and M. Y. Wang, 2023: Internal Variability Increased Arctic Amplification During 1980-2022. *Geophys. Res. Lett.*, **50**, doi:10.1029/2023gl106060.

Swingedouw, D., J. Mignot, P. Braconnot, E. Mosquet, M. Kageyama, and R. Alkama, 2009: Impact of freshwater release in the North Atlantic under different climate conditions in an OAGCM. *J. Climate*, **22,** 6377-6403.

Tan, I., and T. Storelvmo, 2019: Evidence of strong contributions from mixed-phase clouds to Arctic climate change. *Geophys. Res. Lett.*, **46,** 2894-2902.

Tan, I., T. Storelvmo, and M. D. Zelinka, 2016: Observational constraints on mixed-phase clouds imply higher climate sensitivity. *Science*, **352,** 224-227.

Tan, I., G. Sotiropoulou, P. C. Taylor, L. Zamora, and M. Wendisch, 2023: A review of the factors influencing Arctic mixed-phase clouds: progress and outlook. Clouds and Their Climatic Impacts: Radiation, Circulation, and Precipitation, S. C. Sullivan, and C. Hoose, Eds., John Wiley & Sons, Inc., 103-132pp.

Taylor, P. C., and E. Monroe, 2023: Isolating the surface type influence on Arctic low-clouds. J. Geophys. Res., 128, e2022JD038098, doi:10.1029/2022JD038098.

Taylor, P. C., R. C. Boeke, L. N. Boisvert, N. Feldl, M. Henry, Y. Y. Huang, P. L. Langen, W. Liu, F. Pithan, S. A. Sejas, and I. V. Y. Tan, 2022: Process drivers, inter-model spread, and the path forward: A review of amplified Arctic warming. *Front. Earth Sci.*, **9**, doi:10.3389/feart.2021.758361.

Thompson, A. J., J. Zhu, C. J. Poulsen, J. E. Tierney, and C. B. Skinner, 2022: Northern Hemisphere vegetation change drives a Holocene thermal maximum. *Sci. Adv.*, **8,** doi:10.1126/sciadv.abj6535.

Timmermans, M. L., and J. Marshall, 2020: Understanding Arctic Ocean circulation: A Review of ocean dynamics in a changing climate. *J. Geophys. Res.-Oceans*, **125**, e2018JC014378, doi:10.1029/2018JC014378.

Tindall, J. C., A. M. Haywood, U. Salzmann, A. M. Dolan, and T. Fletcher, 2022: The warm winter paradox in the Pliocene northern high latitudes. *Clim. Past*, **18,** 1385-1405.

Tjernström, M., M. D. Shupe, I. M. Brooks, P. Achtert, J. Prytherch, and J. Sedlar, 2019:

Arctic summer airmass transformation, surface Inversions, and the surface energy budget. *J. Climate*, **32**, 769-789.

Tokinaga, H., S. P. Xie, and H. Mukougawa, 2017: Early 20th-century Arctic warming intensified by Pacific and Atlantic multidecadal variability. *Proc. Natl. Acad. Sci. USA*, **114,** 6227-6232.

Thackeray, C. W., X. Qu and A. Hall, 2018: Why do models produce spread in snow albedo feedback? *Geophys. Res. Lett.*, **45**, 6223-6231.

Thackeray, C.W., C. Derksen, C.G. Fletcher and A. Hall, 2019: Snow and climate: feedbacks, drivers, and indices of change. *Curr. Clim. Chan. Rep.*, **5**, 322-333.

Tobo, Y. and Coauthors, 2019: Glacially sourced dust as a potentially significant source of ice nucleating particles. *Nat. Geosci.*, **12**, 253-258.

Tobo, Y. and Coauthors, 2024: Surface warming in Svalbard may have led to increases in highly active ice-nucleating particles. Commun. Earth Environ., **5**, doi:10.1038/s43247-024-01677-0.

Tokinaga, H., S.P. Xie and H. Mukougawa, 2017: Early 20th-century Arctic warming intensified by Pacific and Atlantic multidecadal variability. *Proc. Natl. Acad. Sci. USA*, **114**, 6227-6232.

Tsushima, Y., S. Emori, T. Ogura, M. Kimoto, M. J. Webb, K. D. Williams, M. A. Ringer, B. J. Soden, B. Li, and N. Andronova, 2006: Importance of the mixed-phase cloud distribution in the control climate for assessing the response of clouds to carbon dioxide increase: a multi-model study. *Clim. Dyn.*, **27,** 113-126.

Turney, C. S. M., and R. T. Jones, 2010: Does the Agulhas Current amplify global temperatures during super-interglacials? *J. Quat. Sci.*, **25,** 839-843.

Turney, C. S. M., R. T. Jones, N. P. McKay, E. van Sebille, Z. A. Thomas, C.-D. Hillenbrand, and C. J. Fogwill, 2020: A global mean sea surface temperature dataset for the Last Interglacial (129–116 ka) and contribution of thermal expansion to sea level change. *Earth Syst. Sci. Data*, **12,** 3341-3356.

Uttal, T., and Coauthors, 2002: Surface heat budget of the Arctic Ocean. *Bull. Amer. Meteor. Soc.*, **83**, 255-275.

van der Linden, E. C., D. Le Bars, R. Bintanja, and W. Hazeleger, 2019: Oceanic heat transport into the Arctic under high and low CO_2 forcing. *Clim. Dyn.*, **53,** 4763-4780.

Vavrus, S., 2004: The impact of cloud feedbacks on Arctic climate under greenhouse forcing. *J. Climate*, **17,** 603-615.

Vermassen, F., M. O'Regan, A. de Boer, F. Schenk, M. Razmjooei, G. West, T. M. Cronin, M. Jakobsson, and H. K. Coxall, 2023: A seasonally ice-free Arctic Ocean during the Last Interglacial. *Nat. Geosci.*, **16**, 723–729.

Wang, Q., C. Wekerle, S. Danilov, X. Z. Wang, and T. Jung, 2018: A 4.5 km resolution Arctic Ocean simulation with the global multi-resolution model FESOM 1.4. *Geosci. Model Dev.*, **11,** 1229-1255.

Warren, S. G. and W. J. Wiscombe, 1980: A model for the spectral albedo of snow 2. Snow containing atmospheric aerosols. *J. Atmos. Sci.*, **37**, 2734-2745.

Weiffenbach, J. E., M. L. J. Baatsen, H. A. Dijkstra, A. S. von der Heydt, A. Abe-Ouchi, E. C. Brady, W.-L. Chan, D. Chandan, M. A. Chandler, C. Contoux, R. Feng, C. Guo, Z. Han, A. M. Haywood, Q. Li, X. Li, G. Lohmann, D. J. Lunt, K. H. Nisancioglu, B. L. Otto-Bliesner, W. R. Peltier, G. Ramstein, L. E. Sohl, C. Stepanek, N. Tan, J. C. Tindall, C. J. R. Williams, Q. Zhang, and Z. Zhang, 2023: Unraveling the mechanisms and implications of a stronger mid-Pliocene Atlantic Meridional Overturning Circulation (AMOC) in PlioMIP2. *Clim. Past*, **19,** 61-85.

Westerhold, T., N. Marwan, A. J. Drury, D. Liebrand, C. Agnini, E. Anagnostou, J. S. K. Barnet, S. M. Bohaty, D. De Vleeschouwer, F. Florindo, T. Frederichs, D. A. Hodell, A. E. Holbourn, D. Kroon, V. Lauretano, K. Littler, L. J. Lourens, M. Lyle, H. Pälike, U. Röhl, J. Tian, R. H. Wilkens, P. A. Wilson, and J. C. Zachos, 2020: An astronomically dated record of Earth's climate and its predictability over the last 66 million years. *Science*, **369,** 1383-1387.

Williams, C. J. R., M.-V. Guarino, E. Capron, I. Malmierca-Vallet, J. S. Singarayer, L. C. Sime, D. J. Lunt, and P. J. Valdes, 2020: CMIP6/PMIP4 simulations of the mid-Holocene and Last Interglacial using HadGEM3: comparison to the pre-industrial era, previous model versions and proxy data. *Clim. Past*, **16,** 1429-1450.

Wiscombe, W. J. and S. G. Warren, 1980: A model for the spectral albedo of snow1. Pure snow. *J. Atmos. Sci.*, **37**, 2712-2733.

Wohlfahrt, J., S. P. Harrison, and P. Braconnot, 2004: Synergistic feedbacks between ocean and vegetation on mid- and high-latitude climates during the mid-Holocene. *Clim. Dyn.*, **22,** 223-238.

Wohlfahrt, J., S. P. Harrison, P. Braconnot, C. D. Hewitt, A. Kitoh, U. Mikolajewicz, B. L. Otto-Bliesner, and S. L. Weber, 2008: Evaluation of coupled ocean–atmosphere simulations of the mid-Holocene using palaeovegetation data from the northern hemisphere extratropics. *Clim. Dyn.*, **31,** 871-890.

Woodgate, R. A., 2013: Arctic Ocean circulation: going around at the top of the world. *Nature Education Knowledge*, **4**, 8.

Woodgate, R. A., 2018: Increases in the Pacific inflow to the Arctic from 1990 to 2015, and insights into seasonal trends and driving mechanisms from year-round Bering Strait mooring data. *Prog. Oceanogr.*, **160,** 124-154.

Woods, C., and R. Caballero, 2016: The role of moist intrusions in winter Arctic warming and sea ice decline. *J. Climate*, **29,** 4473-4485.

Woods, C., R. Caballero, and G. Svensson, 2013: Large-scale circulation associated with moisture intrusions into the Arctic during winter. *Geophys. Res. Lett.*, **40,** 4717-4721.

Woods, C., R. Caballero, and G. Svensson, 2017: Representation of Arctic moist intrusions in CMIP5 models and implications for winter climate biases. *J. Climate*, **30,** 4083-4102.

Wu, Y. T., Y. C. Liang, M. Previdi, L. M. Polvani, M. R. England, M. Sigmond and M. H. Lo, 2024: Stronger Arctic amplification from anthropogenic aerosols than from greenhouse gases. *Npj Clim. Atmos. Sci.*, **7**, doi:10.1038/s41612-024-00696-0.

Yamagami, Y., M. Watanabe, M. Mori and J. Ono, 2022: Barents-Kara sea-ice decline attributed to surface warming in the Gulf Stream. Nat. Comm., **13,** doi:10.1038/s41467-022-31117-6.

Yamanouchi, T., 2011: Early 20th century warming in the Arctic: A review. *Polar Sci.*, **5,** 53-71.

Yamanouchi, T., 2019: Arctic warming by cloud radiation enhanced by moist air intrusion observed at Ny-Ålesund, Svalbard. *Polar Sci.*, **21,** 110-116.

Yoshimori, M., and M. Suzuki, 2019: The relevance of mid-Holocene Arctic warming to the future. *Clim. Past*, **15,** 1375-1394.

Yoshimori, M., T. Yokohata, and A. Abe-Ouchi, 2009: A Comparison of Climate Feedback Strength between CO2 Doubling and LGM Experiments. *J. Climate*, **22,** 3374-3395.

Yoshimori, M., A. Abe-Ouchi, and A. Laine, 2017: The role of atmospheric heat transport and regional feedbacks in the Arctic warming at equilibrium. *Clim. Dyn.*, **49,** 3457-3472.

Yoshimori, M., A. Abe-Ouchi, M. Watanabe, A. Oka, and T. Ogura, 2014a: Robust Seasonality of Arctic Warming Processes in Two Different Versions of the MIROC GCM. *J. Climate*, **27,** 6358-6375.

Yoshimori, M., M. Watanabe, A. Abe-Ouchi, H. Shiogama, and T. Ogura, 2014b: Relative contribution of feedback processes to Arctic amplification of temperature change in

MIROC GCM. *Clim. Dyn.*, **42,** 1613-1630.

Zelinka, M. D., T. A. Myers, D. T. McCoy, S. Po-Chedley, P. M. Caldwell, P. Ceppi, S. A. Klein, and K. E. Taylor, 2020: Causes of higher climate sensitivity in CMIP6 models. *Geophys. Res. Lett.*, **47**, doi:10.1029/2019GL085782.

Zhang, P. F., G. Chen, M. F. Ting, L. R. Leung, B. Guan and L.F. Li, 2023: More frequent atmospheric rivers slow the seasonal recovery of Arctic sea ice. *Nat. Clim. Chan.*, **13**, 266-273.

Zhang, P. F., G. Chen, M. F. Ting, L. R. Leung, B. Guan, and L. F. Li, 2023: More frequent atmospheric rivers slow the seasonal recovery of Arctic sea ice. *Nat. Clim. Change*, **13,** 266-273.

Zhang, Q., H. S. Sundqvist, A. Moberg, H. Körnich, J. Nilsson, and K. Holmgren, 2010: Climate change between the mid and late Holocene in northern high latitudes – Part 2: Model-data comparisons. *Clim. Past*, **6,** 609-626.

Zhang, Q., E. Berntell, J. Axelsson, J. Chen, Z. Han, W. de Nooijer, Z. Lu, Q. Li, Q. Zhang, K. Wyser, and S. Yang, 2021a: Simulating the mid-Holocene, last interglacial and mid-Pliocene climate with EC-Earth3-LR. *Geosci. Model Dev.*, **14,** 1147-1169.

Zhang, Z., X. Li, C. Guo, O. H. Otterå, K. H. Nisancioglu, N. Tan, C. Contoux, G. Ramstein, R. Feng, B. L. Otto-Bliesner, E. Brady, D. Chandan, W. R. Peltier, M. L. J. Baatsen, A. S. von der Heydt, J. E. Weiffenbach, C. Stepanek, G. Lohmann, Q. Zhang, Q. Li, M. A. Chandler, L. E. Sohl, A. M. Haywood, S. J. Hunter, J. C. Tindall, C. Williams, D. J. Lunt, W.-L. Chan, and A. Abe-Ouchi, 2021b: Mid-Pliocene Atlantic meridional overturning circulation simulated in PlioMIP2. *Clim. Past*, **17,** 529-543.

Zhang, Z. S., K. H. Nisancioglu, M. A. Chandler, A. M. Haywood, B. L. Otto-Bliesner, G. Ramstein, C. Stepanek, A. Abe-Ouchi, W. L. Chan, F. J. Bragg, C. Contoux, A. M. Dolan, D. J. Hill, A. Jost, Y. Kamae, G. Lohmann, D. J. Lunt, N. A. Rosenbloom, L. E. Sohl, and H. Ueda, 2013: Mid-pliocene Atlantic meridional overturning circulation not unlike modern. *Clim. Past*, **9,** 1495-1504.

Zheng, J., Q. Zhang, Q. Li, Q. Zhang, and M. Cai, 2019: Contribution of sea ice albedo and insulation effects to Arctic amplification in the EC-Earth Pliocene simulation. *Clim. Past*, **15,** 291-305.

Zhong, L., L. Hua, and D. Luo, 2018: Local and external moisture sources for the Arctic warming over the Barents–Kara Seas. *J. Climate*, **31,** 1963-1982.

Zhou, W. Y., L. R. Leung and J. Lu, 2024: Steady threefold Arctic amplification of externally forced warming masked by natural variability. *Nat. Geosci.*, **17**, doi:10.1038/s41561-024-01441-1.

List of Figures

Fig. 4 Illustration of how moisture intrusion may induce Arctic warming through condensation heating and downward longwave radiation from water vapor and clouds. Note that insolation is very weak in the Arctic during winter.

Fig. 5 Estimated global mean surface temperature anomaly (ΔGMST) in ºC: (top) 5 million years ago to present (CE 2000); and (bottom) 1 million year ago to present. Data are originally from Westerhold et al. (2020), Hansen et al. (2013), and Snyder (2016), but later adjusted by Kaufman (2023) for the same reference period (1850-1900).

Fig. 6 Insolation differences among PI (1850), MH (6 ka), and LIG (127 ka): Months in (a) follow celestial calendar which is defined by celestial longitude (angle). The celestial calendar facilitates the interpretation of seasonal comparison at different times, and routinely used in paleoclimate studies. Months in (b) follow modern calendar which is defined by time. In both cases, the vernal equinox is fixed to noon on 21 March. Reproduced from Otto-Bliesner et al. (2017) (Fig. 3, CC BY 3.0).

Fig. 7 Emergent relations in Arctic sea ice cover between past and future simulations: (a) MH vs.CMIP5-RCP8.5 scenario; (b) LIG vs. CMIP6-1pctCO2 experiment. (a) is for September sea ice extent anomaly from PI, and (b) is for summer (June-July-August) sea ice areas. (a) is reproduced from Schmidt et al. (2014) (Fig. 8, CC BY 3.0) and (b) is reproduced from Kageyama et al. (2021) (Fig. 12, CC BY 4.0). The dashed lines are added as a reference for the magnitude of changes, but they are not regression lines. The aspect ratio for (a) was adjusted to display the same sea ice extent at approximately the same length in horizontal and vertical axes.

Fig. 8 Comparison of surface air temperature anomaly to the north of 60ºN between multi-model ensemble means of CMIP6-PMIP4 paleo-simulations (shading) and compilations of proxy-based reconstruction (markers): (a) MH-PI; (b) LIG-PI. Proxy data in (a) are from Sundqvist et al. (2010) and (b) from Turney and Jones (2010). CMIP6-PMIP4 models analyzed are listed in Table 2.

Fig. 9 Simulated vegetation distribution and its impact on surface air temperature anomaly for LIG: (a) simulated vegetation for PI; (b) simulated vegetation for LIG; (c) comparison of simulated temperature anomaly with modern vegetation and proxy reconstruction (LIG-PI); and (d) same as in (c) but including the effect of vegetation change. Figures are reproduced from O'ishi et al. (2021) (CC BY 4.0). In (c) and (d), shadings represent model simulations (MIROC4m and MIROC4m-LPJ) and markers represent proxy reconstructions.

Fig. 10 Comparison of sea surface temperature anomaly of mPWP from PI between a multi-model ensemble mean of CMIP6-PMIP4 paleo-simulations (shading) and a proxy-based reconstruction compilation (markers). The proxy dataset is from Dowsett et al. (2010). CMIP6-PMIP4 models analyzed are listed in Table 2.

Fig. 11 Annual mean potential temperature at 250 m depth (the Atlantic Water layer) in (a) high-resolution model (Kawasaki and Hasumi 2016), (b) 1-degree model, and (c) observation (ProjD). ProjD refers to the dataset constructed by Ishii and Kimoto (2009) and Ishii et al. (2017).

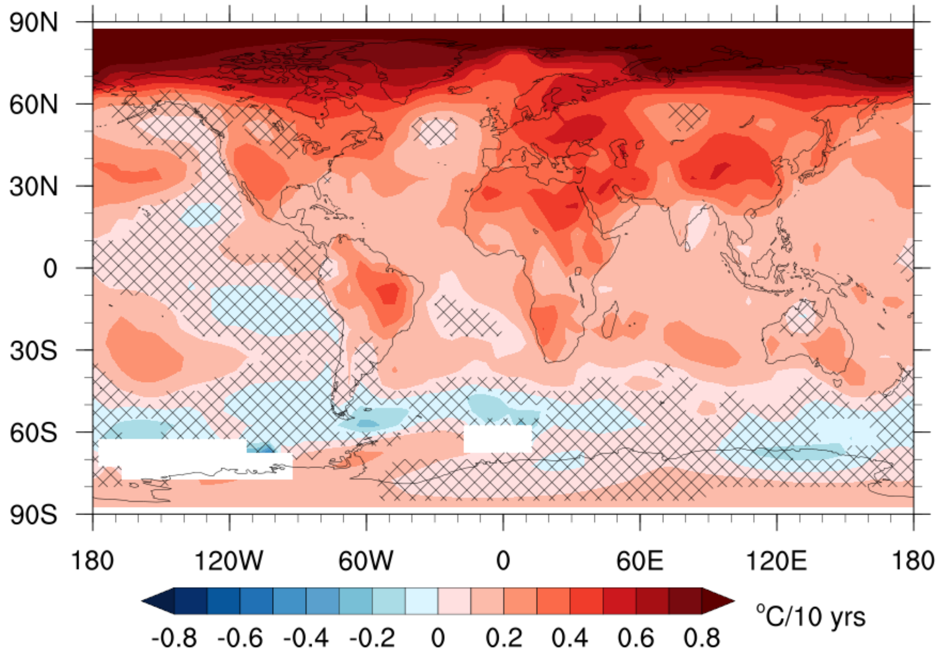

Fig. 1 Linear surface temperature trends from 1979 to 2017 (ºC per decade) after Fig. 2.11 of Gulev et al. (2021). Grid points with missing data are not colored. Grid points where the linear trend is not statistically significant at the 5% level are hatched. The data are from HadCRUT5 (Morice et al., 2021).

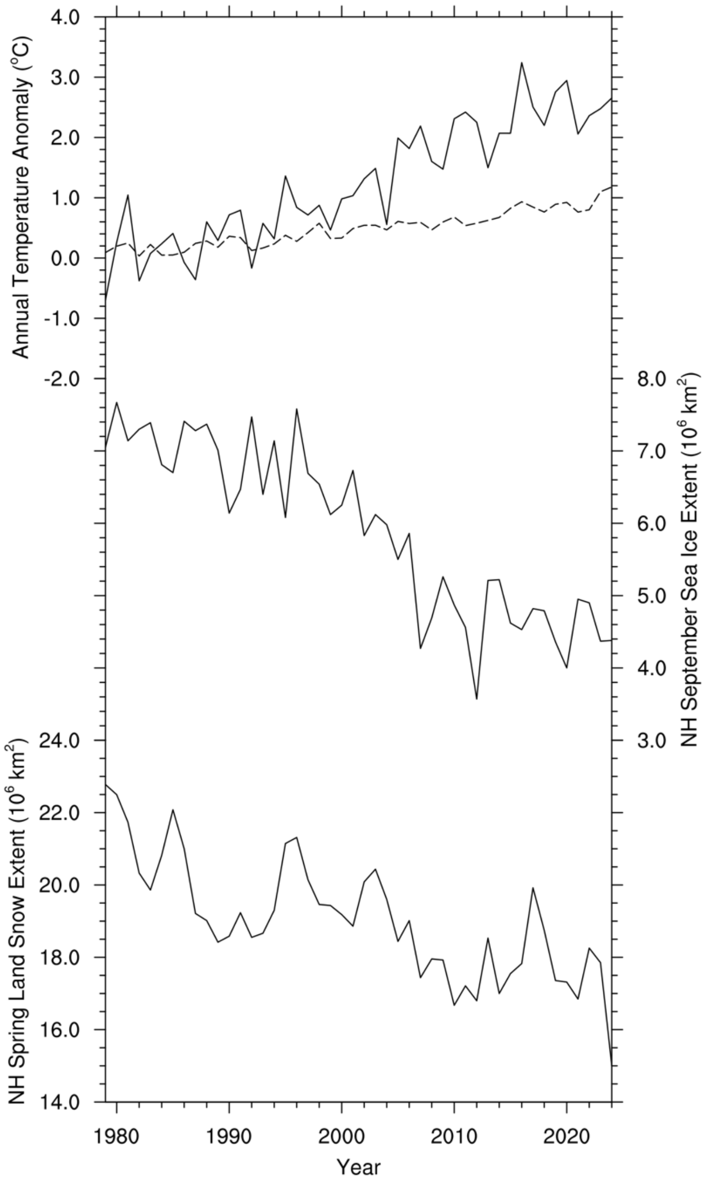

Fig. 2 Time series of (top) annual mean surface temperature anomaly relative to 1961-1990: solid for the Arctic (>66.5ºN) and dashed for the global; (middle) September sea ice extent for the Northern Hemisphere; (bottom) Spring (April-May-June) land snow extent for the Northern Hemisphere. Surface temperature data are from HadCRUT5 (Morice et al., 2021), ice extent data are from NSIDC Sea Ice Index (Version 3), and snow extent data are from Rutgers University Global Snow Lab (Estilow et al., 2015).

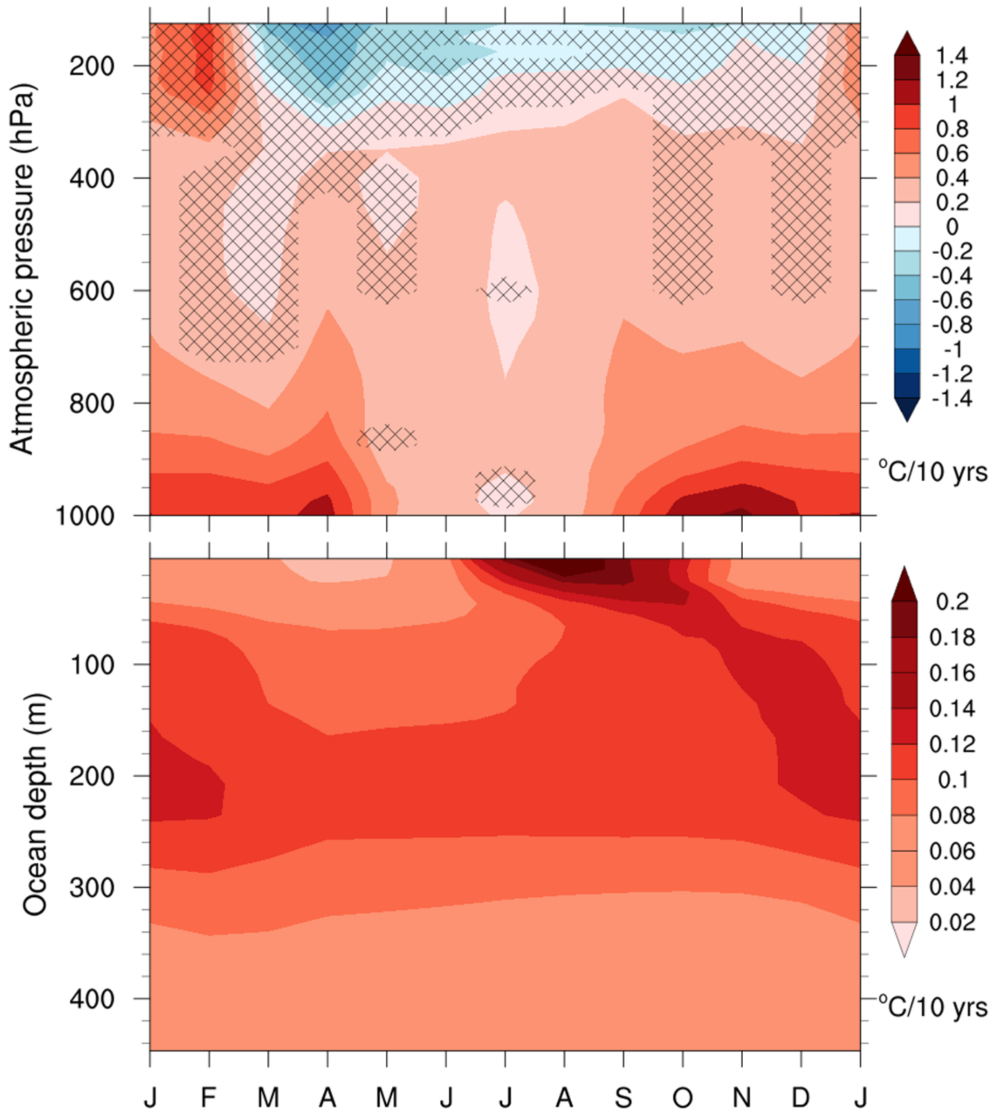

Fig. 3 Linear trends of atmospheric (top) and oceanic (bottom) temperature in the Arctic (average over the region northward of 70ºN) from 1979 to 2017 based on the global reanalysis datasets (ºC per decade). Grid points where the linear trend is not statistically significant at the 5% level are hatched. The atmospheric data are from ERA5 (Hersbach et al. 2020) and oceanic data are from ORA-S4 (Balmaseda et al. 2013).

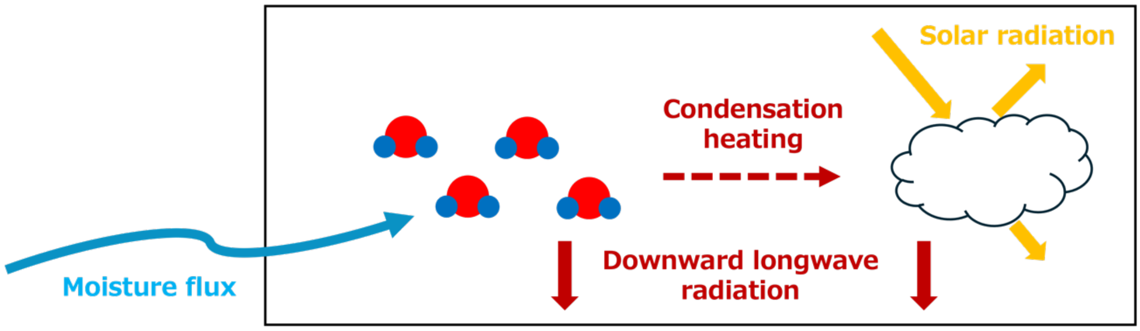

Fig. 4 Illustration of how moisture intrusion may induce Arctic warming through condensation heating and downward longwave radiation from water vapor and clouds. Note that insolation is very weak in the Arctic during winter.

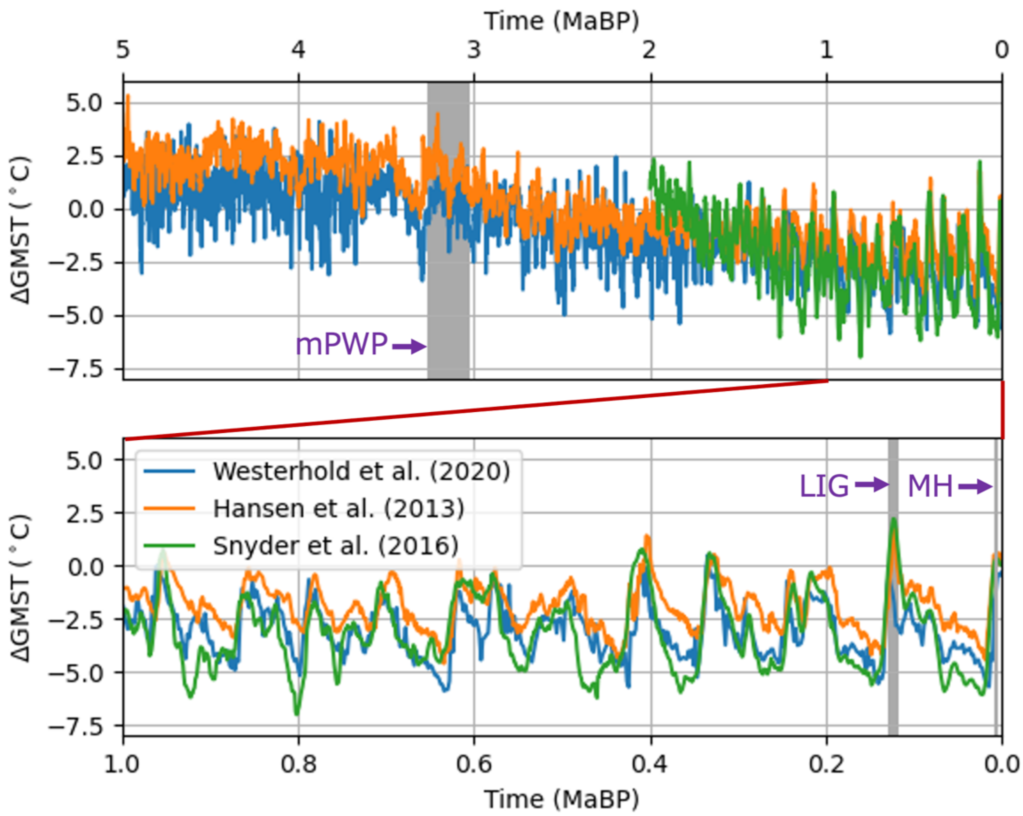

Fig. 5 Estimated global mean surface temperature anomaly (ΔGMST) in ºC: (top) 5 million years ago to present (CE 2000); and (bottom) 1 million year ago to present. Data are originally from Westerhold et al. (2020), Hansen et al. (2013), and Snyder (2016), but later adjusted by Kaufman (2023) for the same reference period (1850-1900).

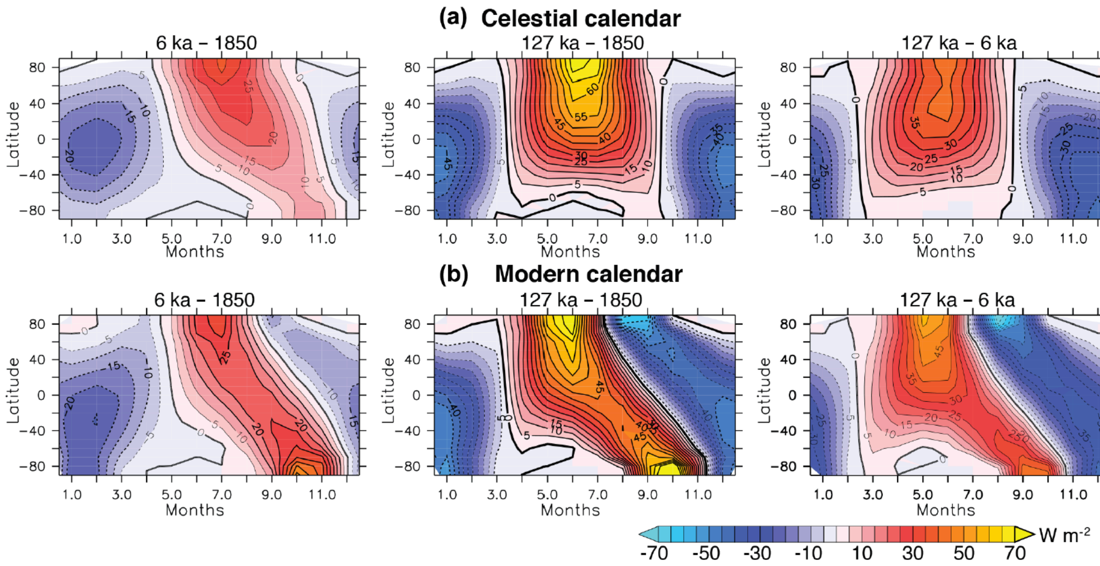

Fig. 6 Insolation differences among PI (1850), MH (6 ka), and LIG (127 ka): Months in (a) follow celestial calendar which is defined by celestial longitude (angle). The celestial calendar facilitates the interpretation of seasonal comparison at different times, and routinely used in paleoclimate studies. Months in (b) follow modern calendar which is defined by time. In both cases, the vernal equinox is fixed to noon on 21 March. Reproduced from Otto-Bliesner et al. (2017) (Fig. 3, CC BY 3.0).

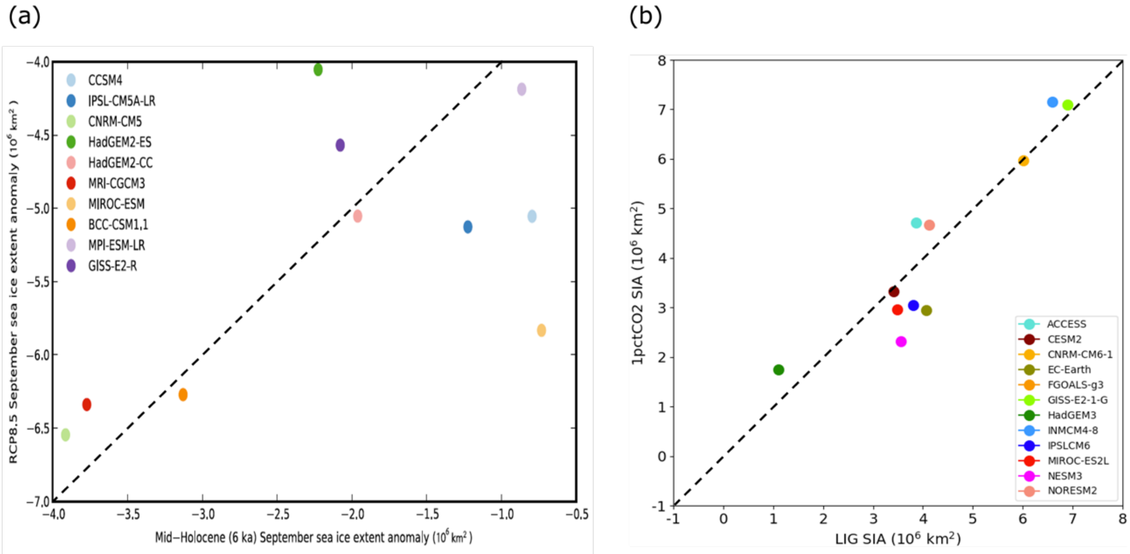

Fig. 7 Emergent relations in Arctic sea ice cover between past and future simulations: (a) MH vs.CMIP5-RCP8.5 scenario; (b) LIG vs. CMIP6-1pctCO2 experiment. (a) is for September sea ice extent anomaly from PI, and (b) is for summer (June-July-August) sea ice areas. (a) is reproduced from Schmidt et al. (2014) (Fig. 8, CC BY 3.0) and (b) is reproduced from Kageyama et al. (2021) (Fig. 12, CC BY 4.0). The dashed lines are added as a reference for the magnitude of changes, but they are not regression lines. The aspect ratio for (a) was adjusted to display the same sea ice extent at approximately the same length in horizontal and vertical axes.

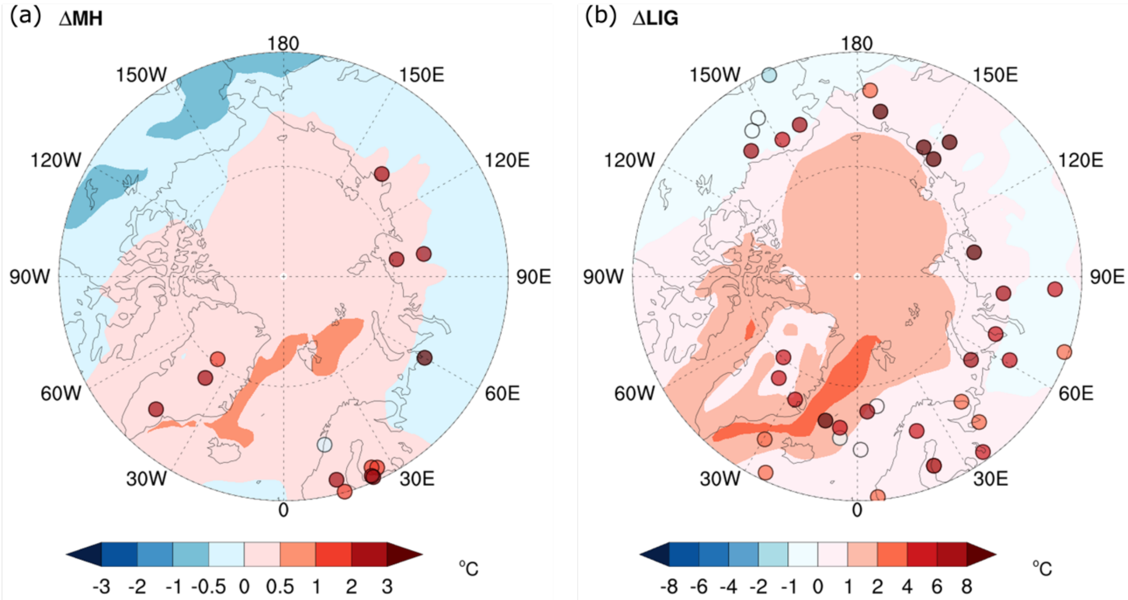

Fig. 8 Comparison of surface air temperature anomaly to the north of 60ºN between multi-model ensemble means of CMIP6-PMIP4 paleo-simulations (shading) and compilations of proxy-based reconstruction (markers): (a) MH-PI; (b) LIG-PI. Proxy data in (a) are from Sundqvist et al. (2010) and (b) from Turney and Jones (2010). CMIP6-PMIP4 models analyzed are listed in Table 2.

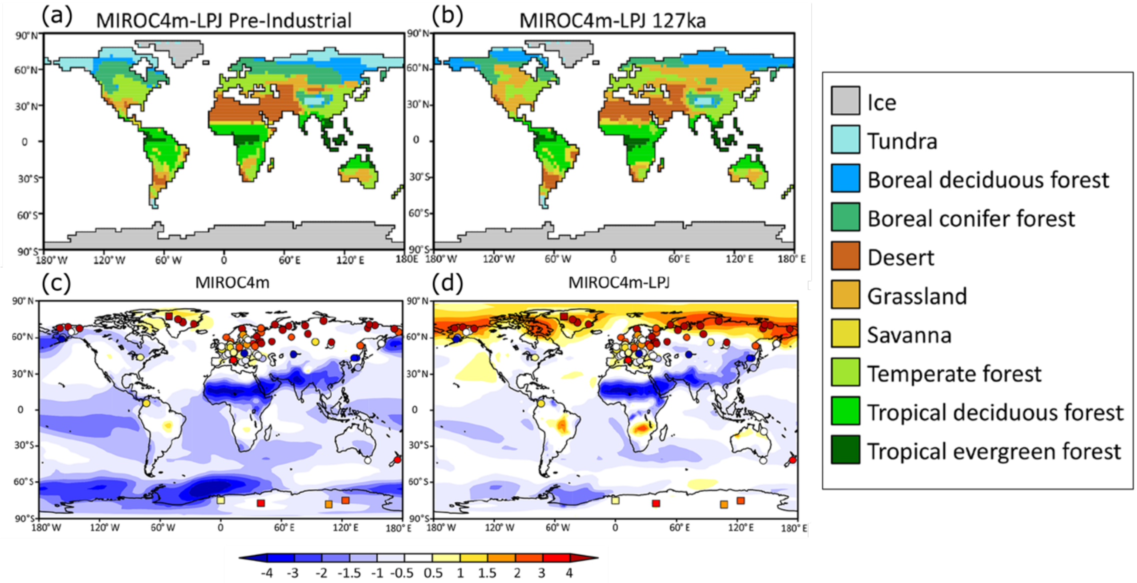

Fig. 9 Simulated vegetation distribution and its impact on surface air temperature anomaly for LIG: (a) simulated vegetation for PI; (b) simulated vegetation for LIG; (c) comparison of simulated temperature anomaly with modern vegetation and proxy reconstruction (LIG-PI); and (d) same as in (c) but including the effect of vegetation change. Figures are reproduced from O'ishi et al. (2021) (CC BY 4.0). In (c) and (d), shadings represent model simulations (MIROC4m and MIROC4m-LPJ) and markers represent proxy reconstructions.

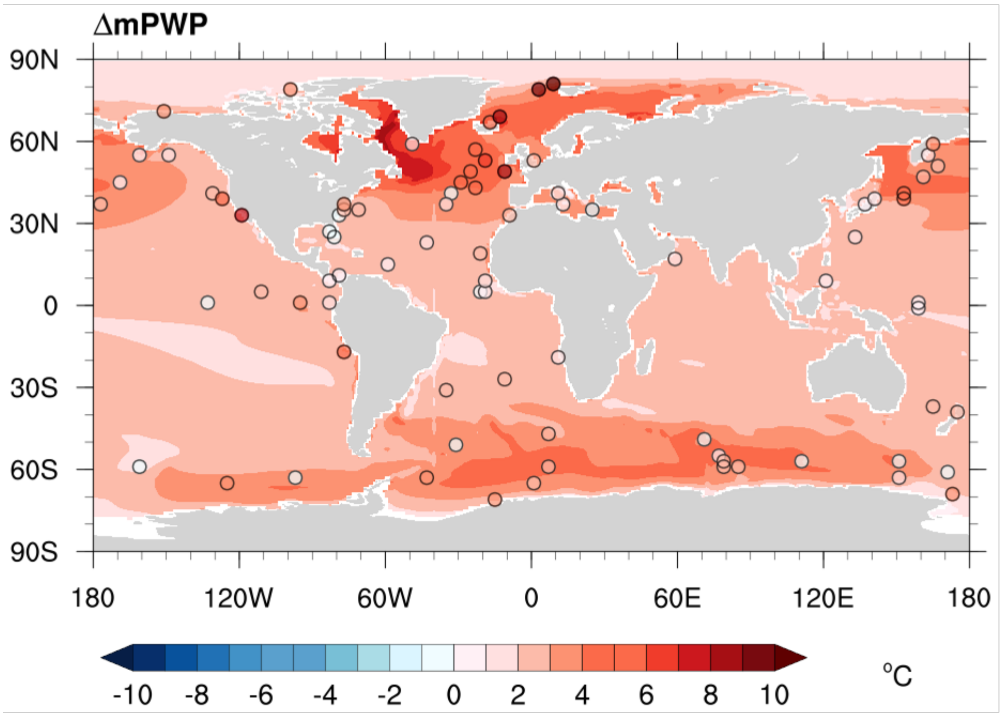

Fig. 10 Comparison of sea surface temperature anomaly of mPWP from PI between a multi-model ensemble mean of CMIP6-PMIP4 paleo-simulations (shading) and a proxy-based reconstruction compilation (markers). The proxy dataset is from Dowsett et al. (2010). CMIP6-PMIP4 models analyzed are listed in Table 2.

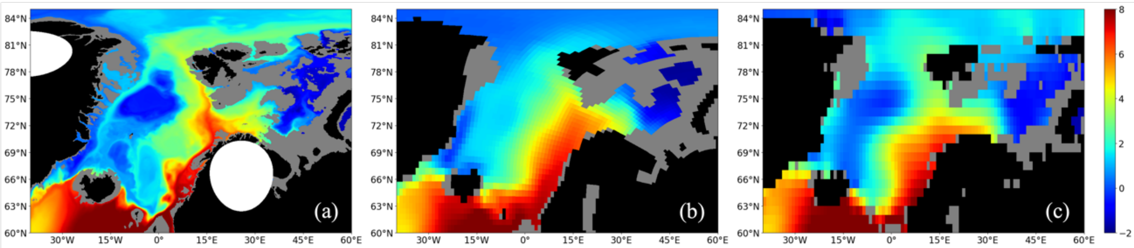

Fig. 11 Annual mean potential temperature at 250 m depth (the Atlantic Water layer) in (a) high-resolution model (Kawasaki and Hasumi 2016), (b) 1-degree model, and (c) observation (ProjD). ProjD refers to the dataset constructed by Ishii and Kimoto (2009) and Ishii et al. (2017).

List of Tables

Table 1 A summary of external forcing specified in the core CMIP6-PMIP4 and PlioMIP2 paleoclimate simulations. Values for PI, MH, and LIG are from Table 1 of Otto-Bliesner et al. (2017), and those for mPWP are from Haywood et al. (2016). [*]See text.

	PI	MH (6 kaBP)	LIG (127 kaBP)	mPWP
Eccentricity	0.016764	0.018682	0.039378	Same as PI
Obliquity (º)	23.459	24.105	24.040	Same as PI
Perihelion - 180 (º)	100.33	0.87	275.41	Same as PI
CO_2 (ppm)	284.3	264.4	275	400
CH_4 (ppb)	808.2	597	685	PI
N_2O (ppb)	273.0	262	255	PI
Geographical conditions				Closed marine channels and reduced ice sheets[*]

Table 2 CMIP6-PMIP4 model output used for the MH, LIG, and mPWP simulations in Figs. 5 and 7. All data are interpolated to 1°×1° (longitude×latitude) grid.

Model name	MH	LIG	mPWP
ACCESS-ESM1-5	✓	✓	
AWI-ESM-1-1-LR	✓		
CESM2	✓	✓	✓
CNRM-CM6-1		✓	
EC-Earth3-LR	✓	✓	✓
FGOALS-f3-L	✓	✓	
FGOALS-g3	✓	✓	
GISS-E2-1-G	✓	✓	✓
HadGEM3-GC31-LL	✓	✓	✓
INM-CM4-8	✓	✓	
IPSL-CM6A-LR	✓	✓	✓
MIROC-ES2L	✓	✓	
MPI-ESM1-2-LR	✓		
MRI-ESM2-0	✓	✓	
NESM3	✓	✓	
NorESM1-F	✓	✓	✓
NorESM2-LM	✓	✓	